



I2 Individual Report

Virtual Wind Tunnel Validation through Wind Tunnel Modification and Experimentation

LUKE BLADES

2014

ECMM102

4th Year MEng Group Project

I certify that all material in this thesis that is not my own work has been identified and that no material has been included for which a degree has previously been conferred on me.

Signed.....

Acknowledgements

This project was performed under the supervision of Dr Gavin Tabor, whom I would like to thank for his support during manufacturing issues. I would also like to thank the University of Exeter, Harrison workshop staff for their assistance in construction.

Abstract

The creation of a (VWT) virtual wind tunnel has the capability to revolutionise automotive design by allowing optimisation through incremental CFD (computational fluid dynamics) analysis. The current industrially accepted method of drag testing, relies on the construction of large clay models for wind tunnel testing. This section of the overall group project was a combination of design, experimentation and analysis, of a wind tunnel test section capable of a fully automated wake survey. This allows for a velocity profile of discrete points for any geometry to be found empirically. A method was also developed for calculating the drag force on the body from this velocity data.

A concept car manufactured using ALM (additive layer manufacturing) was tested in the new wind tunnel test section, whilst a computerized model of the car was tested in identical conditions in CFD. The drag coefficient of the car was calculated in both cases. The virtual wind tunnel drag coefficient was 0.310 and the empirical result was 0.358 ± 0.077 . Since the CFD result was within the error bar of the experimental result, the VWT may be a viable replacement for real wind tunnel testing. However, further experimentation would be required to justify total VWT validation.

Keywords: Wake Survey, Wind tunnel.

Contents

1	Introduction.....	1
2	Project Management.....	2
2.1	Group Structure and Communication between Individual Projects	2
2.2	Time Management and Project Delays	3
2.3	Health and Safety.....	3
2.4	Logbook	4
3	Background and Literature Review.....	4
3.1	Aerodynamic Drag.....	4
3.2	Wind Tunnel Design	5
3.2.1	Open Return Wind Tunnels.....	5
3.2.2	Recirculating Wind Tunnels.....	5
3.2.3	Features of Typical Wind Tunnels.....	6
3.2.4	Use of Wind Tunnels in the Automotive Industry.....	8
3.2.5	Project Wind Tunnel	8
3.3	Theory Used in Data Processing.....	9
3.3.1	Wake Surveys	9
3.3.2	Von Karman's Integral Formulation.....	9
3.3.3	Numerical Integration	10
3.4	Flow Velocity Measurement	10
3.4.1	Pitot-Static Tube Use	10
3.4.2	Velocity calculation from pressure	11
3.4.3	Hot Wire Anemometry.....	11
3.5	CNC (Computer Numerical Control) Positioning Systems.	12
3.5.1	Stepper Motors	12

3.6	Linear Actuators	14
3.7	Motor Control System.....	14
3.7.1	The ‘Raspberry Pi’ Computer	14
3.7.2	Stepper motor Drivers	14
3.8	Flow around a cylinder.....	15
4	Experiment Design and Research Methodology.....	15
4.1	Initial Experiment Design	16
4.2	Final Experiment Design.....	16
4.2.1	Final Experiment Design Methodology	17
4.2.2	Refurbished Tunnel Experiment Set.....	17
4.3	Sustainability	18
4.3.1	Project Energy Consumption.....	18
5	Test Section Design.....	18
5.1	Design Methodology.....	18
5.1.1	Typical Methodologies.....	18
5.1.2	Project Design Methodology.....	18
5.1.3	Project Design Tools.....	19
5.2	Old Test Section Condition	19
5.2.1	Initial State	19
5.2.2	Modifications for Testing.....	19
5.3	New Test Section Design	20
5.3.1	Velocity Measurement Instrument ‘Control Mechanism’ Design.....	20
5.4	Electronic System Design	23
5.4.1	Python Script Design	23
5.4.2	Electronics Hardware.....	23
5.5	Wind Tunnel Section Design.....	24
6	Experimental Methods.....	25

6.1	Gathering Useful data	25
6.2	Initial Experiment Method	25
6.3	Final Experiment Method.....	26
7	Results and Analysis.....	27
7.1	Initial Experiment Findings (old test section)	27
7.2	Final Method Experiment Data Processing.....	29
7.3	Final Method Results Analysis.....	32
7.3.1	Comparison to Drag Balance Experiment.....	32
7.3.2	Tunnel Floor Boundary Layer	33
7.3.3	Comparisons to CFD Data	35
7.3.4	Error Calculation.....	37
8	Future Work.....	38
8.1	Program Development	38
8.2	Further Experimentation for the validation of the VWT	38
8.3	Further Tunnel Improvements	38
8.3.1	Boundary Layer Reduction	38
8.3.2	Smoke Removal.....	38
8.3.3	Turbulence Screen	39
9	Conclusions.....	39
10	References.....	40

1 Introduction

Due to rapidly increasing computer power and the evolution of the automotive industry, the use of computationally aided optimisation will be essential in the design of vehicles with minimised drag coefficients, likely to become popularised by the energy crisis as fossil fuels are depleted and less dense energy sources such as hydrogen become the staple. The current process, used by industry to predict drag (clay modelling and wind tunnel testing), is time and labour intensive. Despite the value of this information to a car manufacturer, this method of testing may become outdated in the coming years. In order to find this information prior to manufacture, often $\frac{1}{4}$ scale (or larger) clay models must be manufactured for preliminary testing. This process is expensive in terms of labour, materials and storage space, but most of all, time. The models are useful for giving approximate results for concept cars early in production, but for processes like optimisation of smaller features, they are close to useless because they are too slow for an iterative analysis. Due to the ease with which CAD (Computer Aided Design) models can be altered, the aim of this project was to prove that CFD (Computational Fluid Dynamics), could be used to create a virtual wind tunnel as a supplementary tool to clay modelling in industry, allowing for optimisation through iterative improvements.

The project had three primary objectives to be achieved by three sub-groups:

- Firstly, a VWT (virtual wind tunnel) would be created with CFD software by the ‘High Performance Computing (HPC) Group’.
- Secondly, a concept car would be designed using CAD by the ‘Design Group’ and tested within the VWT.
- Finally, a real wind tunnel will be modified to give a set of data comparable to those found by the VWT by the ‘Experimental Group’. A 3D printed version of the concept car will be made and tested using the wind tunnel. These results will be compared to the virtual ones to evaluate the validity of the VWT.

The Design group was responsible for designing and manufacturing a concept car alongside a CAD (Computer Aided Design) model. The HPC group was in control of exploring the interaction between mesh structure and turbulence models on solution accuracy and design optimisation through surrogate modelling in CFD software. Once the best meshing strategy and turbulence model had been found, the HPC sub-group was to create a Virtual Wind Tunnel (VWT) using CFD and test the virtual car model made by the design group. The experimental group could then provide a theoretical approximation to the drag of the vehicle with empirical data. This report describes a set of individual research and contributions within the experimental group. Over the course of this project, a wind tunnel test section capable of performing automatic velocity wake surveys was designed, manufactured and tested. This test section consisted of mechanical, electrical and computational sub-systems for automation. A spreadsheet also designed to perform numerous calculations on the raw data obtained from these wake surveys, allowing instant data processing in future experiments.

The report is structured such that chapter 2 will give a summary of the group project structure and the integration of the works of the eight students. Chapter 3 provides an

understanding of the background research on which this individual project was based. This includes studies of existing wind tunnels, measurement equipment and data processing theory as well as a review of previous research in the use of flow measurement equipment and the flow patterns around simple geometries for comparison with project results. The research and methodologies can be found in chapter 4, which also contains a discussion of project sustainability. Chapter 5 describes the design process of the new wind tunnel test section and the design methodology followed to achieve it. Next, the experimental methods for both preliminary and final tests are described in chapter 6. The results of these experiments and their implications are analysed in chapter 7 and chapter 8 describes the recommended further experimentation and tunnel modifications. Finally, the conclusions of the project can be found in chapter 9 and any cited references are detailed in chapter 10.

2 Project Management

This section explains the structure and time management of this individual project, as well as the way in which it was integrated into the VWT group project. It also details the reasons for the time delays which led to incomplete wind tunnel experimentation.

2.1 Group Structure and Communication between Individual Projects

Eight students were divided into 3 sub-groups to work in different areas of the project. These were the HPC (High Performance Computing) group, Design group and Experimental group. The experimental group had interactions with several members of other groups to ensure that the results of all three were compatible.

Firstly, the size of the physical wind tunnel used has a direct effect on the required size of tested geometries, as discussed in section 7.1. This, among other information was conveyed to the design group to aid in the design of a concept car which was fit for testing in the available tunnel. Similar information was communicated to the HPC group, who used the CAD wind tunnel geometries and flow parameters which were supplied by the experimental group, ensuring comparability and cohesiveness. Also when the final experiments were performed, the initially designed experimental technique was compromised, as described in section 6. Information regarding the improvised test conditions was conveyed to HPC.

This information was communicated through two primary media:

1. The use of social media became the first line of communication for updates, questions, small issues and reminders. A private group was created of which, all project members were members. This was especially useful in reducing delays as many group members were instantly accessible via smartphones. Email was also available but tended to have slower response times in general, so social media posts became the norm.
2. Weekly meetings have been held which aided in everything from the establishment of the project objectives to the monitoring of progress throughout the group. Before each meeting, every group member reads through and confirms the minutes of the previous meeting and has the opportunity to add items to the agenda of the following meeting. The supervisor of the project, Gavin Tabor, has attended all

weekly group meetings to ensure that it is on track and to offer advice for future research. Each meeting has an assigned chair and secretary; these roles rotate week by week so the workload is shared. The chair is responsible for creating the agenda and runs the meeting, moving from item to item until all issues for that week are resolved. The secretary is responsible for taking the minutes for that meeting in a minute book and typing up the minutes making them available to the rest of the group before the following meeting. Long term or complex inter-subgroup requirements were discussed in weekly group meetings rather than through social media as it reduced the chance for errors in communication and ensured that all group members were aware of the progressions. The frequency of group meetings also increased dramatically during times at which group deliverables (G1 and G2 reports) were due, to improve the cohesiveness of the activity.

2.2 Time Management and Project Delays

Time was managed throughout the project through the use of ‘Microsoft Project’ to create a Gantt chart which was followed and updated when necessary. It helped to ensure that certain processes were given enough time and was structured to ease the completion of time sensitive work. This was achieved through the use of critical path analysis, in which activities crucial to the completion of the project are prioritised allowing the fastest progress [1]. The initial project plan can be found in appendix 1 for comparison with actual project developments.

Unfortunately, a number of unavoidable time delays were experienced throughout the project. Most notably, the inability of the experimental group to access the workshop for more than just 18 hours, during a 6 week period throughout February and March 2014. The specifics of these delays can be found in appendix 2 ‘Mitigation Application’. The consequences of the time delays are discussed later in this report.

2.3 Health and Safety

This project posed a wide variety of risks due to its practical nature. Health and safety was constantly considered whilst working in the workshop and the fluids laboratory. A risk assessment was performed for all practical activity and remedial action was taken for any risks which were considered to require it, as shown in table 1 and explained in table 2.

Table 1 – Table of Risks and control measures, along with scores of likelihood and severity (1 is low, 5 is high)

Hazards	Existing control measures	Score A	Score B	Risk (A x B)
Sharp airborne metal from spinning tools in workshop (Drill, lathe, milling machine etc) Danger to eyes.	Perspex guards for automatic machines and lathes. Wearing provided goggles in workshop	2	1	2
Accidental touching of moving sharp tools, cutting skin.	Wearing Gloves when working close to blades.	3	1	3
Mild electric shock when wiring computer system	Insulated wires, disconnecting power.	3	1	3
Damage to ears through extended presence of active wind tunnel when taking manual measurements.	Ear protection provided. Taking regular breaks from long experiments	1	1	1
Shrapnel from solid objects hitting the fan in wind tunnel	Mesh screen in front of fan section. Standing clear of tunnel outlet. Regular checks that inlet and tunnel are clear before switching on.	1	3	3
Burning eyes during welding	Welding masks available for welders.	1	3	3

Table 2 – Key for scores given in table 1

Likelihood of injury	Score A	Severity of injury	Score B
improbable	1	very minor injury; abrasions / contusions	1
remote	2	minor injuries; cuts / burns	2
possible	3	major injuries; fractures / cuts / burns / damage to internal organs	3
probable	4	severe injury; amputation / eye loss / permanent disability	4
likely	5	death	5

These and other health issues related to chronic health problems and long term computer use have been considered in the CEMPS Health and Safety form given in appendix 3.

2.4 Logbook

A logbook was kept as a project management tool to keep track of progress, group work and for rough design work. It was used to store part drawings to consult during workshop hours and during the highly iterative design process, was used to record thoughts, ideas and sketches for further development. Finally the logbook was used to record minutes specific to this personal project and to the experimental group.

3 Background and Literature Review

The background section of this report provides an understanding of the theories and equipment used during the project. It also explains the importance of this research to automotive design and to the environment.

3.1 Aerodynamic Drag

This is defined as the resistive force experienced by a solid body against its direction of motion (or in the direction of the flow), by a fluid in relative motion [2]. This applies both to bodies in a wind tunnel, in which the flow is moving over the body and also to bodies in motion through fluids. From the drag force, flow properties and body geometry, a drag coefficient ‘ C_D ’ can be calculated, which is a dimensionless quantity, allowing comparisons of drag between bodies of different scales. Automobile drag coefficients vary greatly, however for cars, the average falls between 0.27 and 0.31 [3]. Throughout this project, the drag coefficient of the concept car was the quantity used for comparison between experimental techniques and CFD results. The formula for calculating the drag coefficient of a body is given in equation 1

Equation 1: Drag Coefficient [4]

$$C_D = \frac{F_D}{0.5 \times \rho U^2 A}$$

Where F_D is drag force, ρ is fluid density, U is free stream velocity and A is the frontal area of the body, perpendicular to the direction of the flow.

3.2 Wind Tunnel Design

The use of wind tunnels in the automotive industry is common. The basic structures of wind tunnels are very similar from model to model, however there is a variety of equipment available for wind tunnel experimentation. This makes them very versatile, both in the geometries of bodies which can be studied within them and the types of data which can be obtained through their use. Generally, wind tunnels can be split into two groups. The first group is ‘Open Return’ tunnels which tend to be smaller and used for education and undergraduate research purposes due to their lower cost and simple maintenance and manoeuvrability. The second group is “Recirculating” tunnels which recycle air within their structure rather than around it. This produces less turbulence and requires less energy to run as the momentum in the flow is conserved rather than dissipated.

3.2.1 Open Return Wind Tunnels

The standard composition of an open return tunnel is shown in figure 1 (right). The bell mouth is wide and designed to allow a gradual acceleration of air into the tunnel to lower turbulence. The next section through which the air passes is called the test section and was the section of the tunnel redesigned during this project. The test section is where any bodies are placed for testing and it usually has at least one transparent side to allow for the use of flow visualisation techniques. The third section of the tunnel is known as the diffuser and is designed to gradually decelerate the flow and raise the pressure. This reduces the amount of power required to maintain velocity in flow [5]. The final common component in open return tunnels is the driving fan. This is used to pull air through the tunnel and well-designed fans can improve the velocity profile of the flow.

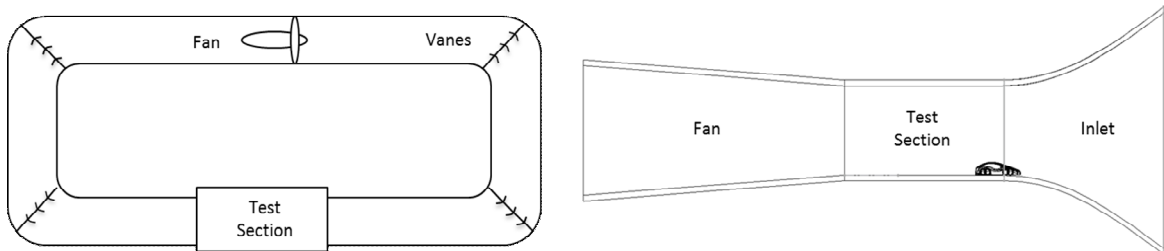


Figure 1 - Recirculating (Left) and Open Return (Right) Wind Tunnel Diagrams [6]

3.2.2 Recirculating Wind Tunnels

Recirculating wind tunnels are more commonly used in industrial research and development. They are large and often built into research buildings. As shown in figure 1 (left) the flow moves in a circuit which both maintains momentum and a more constant velocity profile. The sets of vanes located at the turning points in these tunnels dramatically reduce turbulence. The following points are some of the advantages held by recirculating tunnels over open return. During this project, measures were taken to overcome some of these issues in the open return tunnel used for testing.

- Industrial tests are often on a very large scale (cars, aircraft etc.). Accelerating the flow requires a large propeller hence considerable usage of energy. A recirculating tunnel prevents as much energy being lost, open return tunnels must accelerate all

flow from zero to the required freestream velocity. This does not conserve momentum and results in higher turbulences.

- Recirculating tunnels can use a comparatively small propeller to drive their flow as the fluid can be passed through it several times to achieve required velocities since momentum is conserved, the only losses are through viscous forces. This requires that the tunnel is allowed a few seconds to get to speed. With open return tunnels, the flow only passes over the propeller once before being ejected into the atmosphere, so it must reach the required velocity in a very short space (between the bellmouth and test section). This again increases energy requirements but more notably, the noise. This potentially limits the use time of such tunnels in avoidance of noise pollution. The ability to use the test section built during this project at night is key to obtaining certain data sets.
- The largest advantages of recirculating tunnels are obviously due to performance improvements. This is especially true for industrial research in which the costs of noise and energy consumption would be vastly outweighed by the value of the data obtained. The flow in open return tunnels has a very short distance over which to accelerate to freestream velocity. Also the velocity profile of the flow entering the bellmouth may be non-uniform due to the geometry of the room or object obstructing flow to certain areas. This may be the case for the tunnel used for this project as the inlet was close to a wall with a desk obstructing part of the flow as shown in figure 2, the smoother, less turbulent flow in recirculating tunnels is likely to give better results.

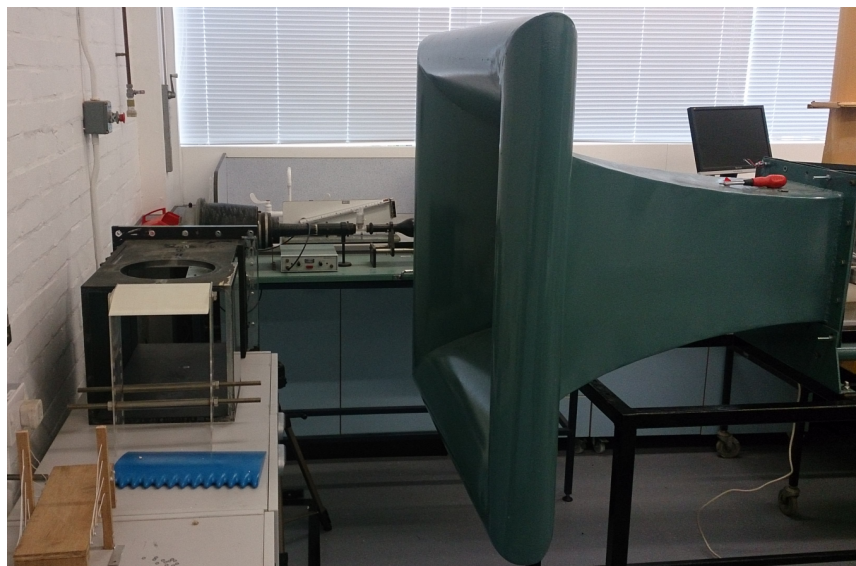


Figure 2 – Photograph to show the proximity of the project tunnel inlet to obstructions at the time of experimentation

3.2.3 Features of Typical Wind Tunnels

The use of wind tunnels in the design process of automobiles is invaluable to manufacturers. Modern tunnels can be used in a variety of ways with a number of flow and force measurement systems to provide information which currently cannot be reliably found using CFD. Examples of modifications which can be made to increase the realism of the testing are described below.

3.2.3.1 Boundary Layer Reduction

It was proven by Ludwig Prandtl that the flow around a body could be split into two theoretical regions. The first of which being a thin layer surrounding the body which is strongly influenced by the viscosity of the fluid, whilst in the region outside of this layer, viscosity can be neglected. [7] The boundary layers on the wall surfaces of the tunnel are one of the key inaccuracies in the usage of wind tunnels. These are the regions close to the wall where the flow is slowed due to the viscous interactions.

When considering automotive design, having the car drive through the flow and moving the flow over the car are not equivalent, as the latter results in the lower portion of the vehicle experiencing boundary layer flow (reduced velocity). To remedy this, some wind tunnels use systems to reduce or eliminate the boundary layer on the floor of the tunnel. Boundary layer reduction was not applied to the wind tunnel in this project, however it has been recommended, that it may be possible as a future modification to the tunnel and may heavily impact wake survey results. The effects of the boundary layer on the experimental results are discussed in section 7.3.2 and the most suitable methods for reducing the boundary layer in the project tunnel are discussed in section 8.3.1.

3.2.3.2 Climate Control

Due to the variation in fluid viscosity with temperature, full scale industrial wind tunnels are often equipped with thermal control to gain further control of test conditions. This can be important for testing the performance of the car in different environments, however its main use is in the testing of engine cooling systems. Full scale cars are tested in flow speeds up to 275 km/h and 50°C to prove that the engine can be cooled beyond realistic requirements. [8]

3.2.3.3 Flow Visualisation

This is a qualitative form of flow analysis often used in design as it provides graphic representation of flow patterns to designers. This is often easier to perform and analyse than the qualitative methods discussed and can shorten lead times in design projects. It is especially useful in the early stages of projects, as is possible to visually identify the origins of vortices or boundary layer separations. The technique currently available for use in the project tunnel is smoke visualisation. This consists of feeding smoke into the flow at a position upstream of the tested model and observing the flow of smoke over the body. The smoke can be formed of vapours but is usually composed of combustion products. Modern smoke generators rely on the vaporisation of hydrocarbon oils, specifically kerosene [9]. This produces a bright white smoke which provides vivid visualisation, however is considered dangerous to inhale in large doses.

The removal of the smoke from the flow downstream of the body serves different purposes depending on the type of wind tunnel being used. In recirculating tunnels, if the smoke is not removed from the flow, then it will stay in the system and accumulate. This lessens the effectiveness of the visualisation as the flow becomes more clouded. On the other hand, in open return tunnels like the project tunnel, the smoke is blown by the fan into the laboratory. Over time this will accumulate and can endanger anyone working in the lab.

3.2.4 Use of Wind Tunnels in the Automotive Industry

Wind tunnels are key in the design process of the automotive industry. The increasing rarity of fossil fuel deposits along with increasing demand for energy raises the importance of fuel efficiency in vehicular design from the perspective of both the consumer and the environment. When high energy density fuels such as petrol and diesel have been depleted, hydrogen is likely to become the main automotive fuel. H₂ can be produced by electrolysis of water, powered by solar or wind energy, which makes it renewable, however it has very low energy density even when pressurised or liquidised. Consequently, improving the energy efficiency of a hydrogen vehicle will:

- Increase the distance the car can travel without the need to refuel
- Decrease the running costs
- Improve performance – Less fuel will be required on-board and a lower vehicular mass results in lower rolling friction, less energy loss during braking.

This places pressure on the automotive industry to create cars in which fuel efficiency is not only improved, but optimised. Although the theoretical fluid dynamics theory is available for the use of CFD for single simulations to an industrially accepted level of accuracy, the hardware required to perform these calculations is expensive, large and although powerful, can still take weeks to run a single simulation. As a result, it is not viable for optimisation in which many similar simulations must be run to obtain the best possible design configuration. Wind tunnels are often used for wake surveys and streamline analysis using flow visualisation. This is performed on clay model cars.

3.2.5 Project Wind Tunnel

The Photograph in figure 3 shows the wind tunnel used in this report, referred to here as the ‘project wind tunnel’. It is situated in the university fluid dynamics laboratory and is open return in design. The maximum flow velocity recorded was approximately 45 ± 3 m/s. This flow speed can be altered through the use of the velocity control fins at the outlet of the tunnel.

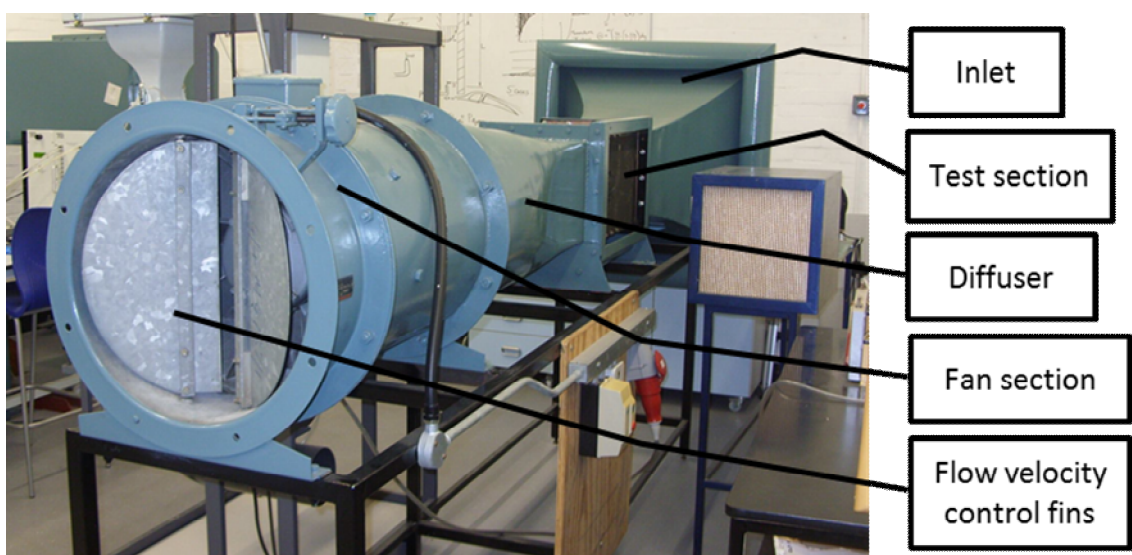


Figure 3- Photograph of the project wind tunnel driving unit (right), and Inlet section (left). The section connecting these two was the test section (redesigned in this project).

3.3 Theory Used in Data Processing

3.3.1 Wake Surveys

The wake in a fluid is the region affected by a body in relative motion to the flow. In wind tunnel testing, this is directly downstream of the body being tested. A wake survey is an experiment designed to find a certain quantity (velocity, temperature, pressure etc) across the whole wake in a plane downstream of a body in a wind tunnel. The required complexity of this experiment depends on the geometry of the body. In this project, wake surveys of pressure were performed. There is no definitive method for performing a wake survey and several parameters must be chosen based on the use of the required data.

Certain calculations (including momentum loss calculated in this report) require that the wake ‘data plane’ can be split into small areas, so it makes sense to measure the wake at regular intervals to produce a grid of equal areas. Conversely, if the wake were expected to be uniform or to have a pattern, then evenly spaced data could be misleading and cause systematic errors, and a degree of randomness may be required. If a regular grid is chosen, then the distance between data points, also known as the ‘resolution’, will influence both the accuracy of the survey and the amount of time taken to complete it.

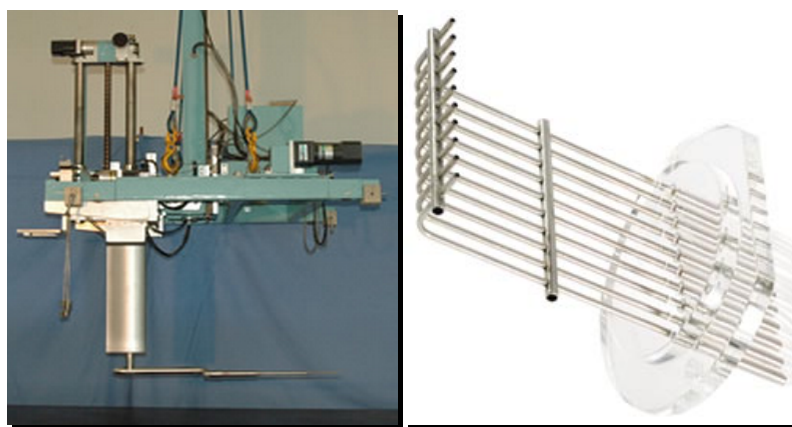


Figure 4- Example of a commercial measurement instrument positioning system (left) [10] and a Pitot tube array (right) [11]

To ensure accurate positioning, some form of support rig for the measurement instruments is often utilised. Industrial systems such as that shown in figure 4 (left), are able to move a Pitot tube in three dimensions so that multiple wake surveys, at varying distances from the body, can be taken automatically. Other more simple systems use an array of Pitot tubes, called a ‘rake’, to take multiple readings at once, exemplified in figure 4 (right). This allows many more measurements to be taken in a set amount of time. Also if the rake is wide enough to cover the whole wake and the gaps between the Pitot tubes are small enough, then the rake will not need to be moved in that direction, simplifying the system.

3.3.2 Von Karman's Integral Formulation

Fluid within a wake moves at a different speed or in a different direction to the free stream, and consequently has a different momentum (Momentum = Velocity x Mass). Due to the principle of conservation of linear momentum, the change in momentum experienced by the entire wake in any cross sectional plane perpendicular to the direction of the free stream will be equal to the aerodynamic drag force on the body in the flow ($F = ma$). To

find this change in momentum, the momentum flux across a plane in the flow encompassing the entire wake is either measured or calculated using experiments or CFD.

Equation 2: Von Karman Integral Formulation [12]

$$\frac{F_D}{L} = \rho \int_0^y U_x (U_\infty - U_x) dy$$

Where U_x is wake velocity, U_∞ is free stream velocity, y is the distance from start of control volume and F_D is the drag force.

Consider a prismatic shape (uniform cross section), of infinite length and uniform flow perpendicular to its length. Equation 2 is an application of the Von Karman momentum conservation principle to find the momentum loss per unit length, of a control volume of height ‘y’.

3.3.3 Numerical Integration

3.3.3.1 Application of Von Karman's to Discrete Data

Von Karman's integral formulation is typically used in situations where the velocity of the wake can be approximated as function of its position in Cartesian or polar coordinates. For bodies whose wake is unknown this is not possible, however if data is obtained at small intervals and the control volume is discretised, then numerical methods can be employed to find the loss of momentum in the flow, which is equal to the drag force on the body. During this project, numerical methods were developed which allowed the use of Von Karman's to analyse one and two-dimensional data sets.

3.3.3.2 Trapezium Rule for One-Dimensional Data Analysis

If a body is prismatic in any plane and is oriented correctly in the wind tunnel, then the data for the entire wake can be measured by taking a one dimensional line of data points. This is because the wake will also be prismatic and therefore the pressure can be assumed equal at any cross section of its length. This is assuming that the data is taken sufficiently far from the end of the body such that the effects of its ends do not influence the results. The trapezium rule is a numerical method which assumes that the flow velocity varies linearly between adjacent data points. The area under this graph is summed in the application of Von Karman integral formulation to find the total drag on the body.

3.4 Flow Velocity Measurement

Flow velocity can be measured in a number of ways. Depending on the method, the raw data obtained from the flow may need to be processed to give velocity data.

3.4.1 Pitot-Static Tube Use

A Pitot tube is a hollow tube pointed into a fluid flow in order to measure the pressure at that point. The tube is connected to a manometer and the pressure at this point in the flow can be read from the scale. At the tip of the tube, a “stagnation point” develops where the

pressure within the tube matches that out the outside and in theory the fluid at this point is in equilibrium and becomes stationary.

A basic Pitot tube only has one hole at the tip, directed parallel to the flow. This is used to measure total pressure. As discussed in section 7.2, both the total pressure and static pressure are required to calculate flow velocity. Therefore, often slightly more complex instruments called “Pitot-static” tubes are used when velocity and not just pressure is being measured. Pitot-static tubes have a secondary port on the side which is perpendicular to the flow. Consequently, there is no velocity component in the direction of the entrance to this second port and the pressure inside is unaffected by the kinetic energy in the flow. This pressure is equal to the static pressure “ P_s ” in the flow, which is the pressure experienced by a body if the flow were stationary, or if the body moves at the same rate as the flow. Therefore, a Pitot-static tube took measurements of both the total pressure and the static pressure.

3.4.2 Velocity calculation from pressure

Bernoulli’s theorem is used in the calculation of flow velocity using pressure measurements. It states that energy along a streamline in a flow remains constant or more specifically, the sum of the static pressure, kinetic pressure and gravitational potential energy (head) is constant. This is expressed mathematically in equation 3.

Equation 3 – Bernoulli’s Equation [12]

$$\frac{\rho v^2}{2} + P_s + \rho gh = P_t$$

Where P_s is static pressure, P_t is total pressure, g is the gravitational constant, h is height, v is velocity and ρ is fluid density.

Applying this theorem to the calculation of velocity from Pitot-static tube data, the potential energy term (ρgh), can be neglected as there is no difference in height between the 2 ports on the tube. Therefore, if static and total pressures are measured using a Pitot-static tube, then the flow velocity becomes the only unknown variable and the equation can be rearranged to give equation 4, with velocity as the subject.

Equation 4 – Equation to determine flow velocity from Pitot-static tube measurements.

$$v = \sqrt{\frac{2(P_t - P_s)}{\rho}}$$

3.4.3 Hot Wire Anemometry

This was the second flow measurement technique used in the initial experiments. Hot wire anemometry relies on the relationship between fluid velocity and rate of convection from a stationary object in the flow to the fluid. The anemometer consists of a probe and a

computer. Often a data logger is used in tandem to increase the accuracy of the results. [13]

The probe consists of two electrodes, bridged by a piece of wire only several microns in diameter. During testing, the probe is heated to a few degrees above ambient temperature, so as fluid flows past the probe, the heat is convected away. The faster the flow, the higher the rate of convection. Voltage across the probe is kept constant and resistance in a wire decreases in proportion with the loss of temperature. Consequently, through the combined use of Ohm's law and Newton's law of cooling, the computer can calculate estimates for the velocity of the flow. Further information of hot wire anemometry can be found in the I1 report [21].

3.5 CNC (Computer Numerical Control) Positioning Systems.

CNC systems are used to accurately and automatically control the position of tooling or measurement equipment in machines like Lathes, Mills and 3D printers. These systems consist of two key sub-systems.

1. Mechanical positioning system capable of moving to required positions with low tolerances and at given speeds.
2. A Computer system with software to define the path of the positioning system (along with some interface to the positioning system).

3.5.1 Stepper Motors

Structurally and conceptually, stepper motors are similar to standard electric motors. They consist of a cylindrical core which spins on the central axis and is driven by electro-magnetised coils which surround the core.

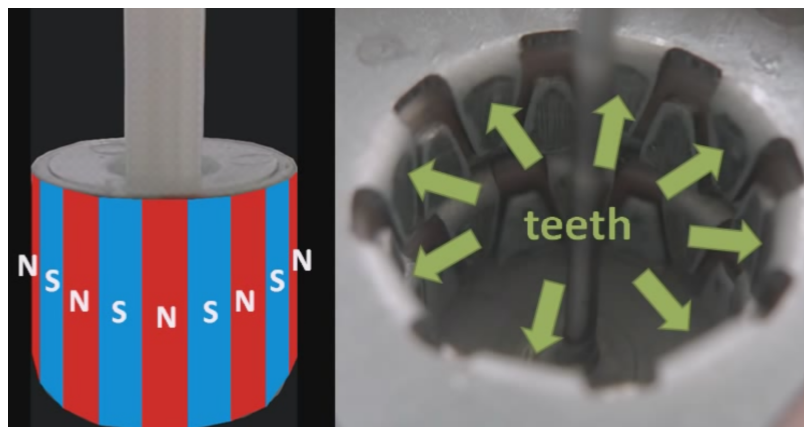


Figure 5 – Figure showing the magnetic arrangement of a stepper motor core (left) and the positions of the teeth on the outer coils [14]

The motion of a stepper motor is in small discrete movements called "steps" rather than continuous spinning. This difference makes stepper motors less appropriate for high speed applications but more well suited for CNC as their movement can be controlled to fine tolerances and they will hold their position against external forces with maximum torque when stationary. This is important in CNC milling machines where steady motion and

accurate positioning are crucial, whilst speeds must be controlled to avoid damage to the tooling. Figure 5 shows the arrangement of both the permanent magnetic poles on the core (Left) and the electromagnetic teeth arranged on 2 coils (Right). The two coils are powered in a certain order and direction to drive the core.

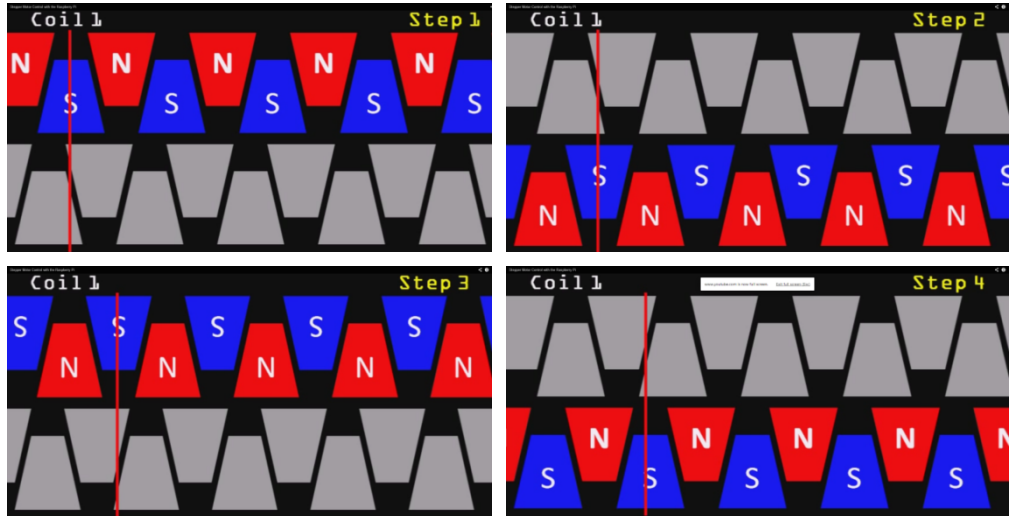


Figure 6: Diagram displaying the 4 key stages of stepper motor operation [14]

The red line in each of the 4 images in figure 6 represents the position of a north pole on the core with respect to the outer coils. The following four steps are repeated to drive the stepper motor:

1. Current is passed through coil 1 in the anti-clockwise direction, creating a magnetic field around the teeth with the north pole facing upwards perpendicular to the coil and the south pole facing downwards. This pulls the core to align its north poles with the downward facing teeth on coil 1.
2. Coil 1 is now switched off and coil 2 is powered in the opposite sense, in the clockwise direction. Consequently the core now rotates through a small angle to align its north poles with the upper teeth on coil 2.
3. Coil 2 is switched off and coil 1 is now powered clockwise, rotating the core to align the north poles with the upper teeth on coil 1.
4. Finally, Coil 1 is switched off and coil 2 is powered anti clockwise to cause another rotation in the core.

The stepping pattern described is only the simplest of the many possible patterns. For example, the “duel stepping” pattern increases motor torque at the cost of increased power consumption by making constant use of both coils in the same order shown in figure 6, but 2 steps at a time (12 , 23 , 34 , 41). This increases the force with which the core is being turned as there are two coils simultaneously generating magnetic fields.

Stepper motors are a popular choice in CNC machines due to their repeatable accuracy in movement without the need for any feedback system. Since the motor responds exactly to the driving signal, it can be assumed that the system is in the right place without checking, although for the sake of error proofing, CNC systems using stepper motors often have simple sensors to ensure that the starting position of the system is correct.

3.6 Linear Actuators

Linear actuators differ from stepper motors in that their motion is continuous. They are usually composed of an electric motor and a lead screw assembly to convert the rotational motion to a linear action. Thanks to their continuous motion, they are capable of moving at much faster speeds than stepper motor systems, which cannot build momentum during motion.

3.7 Motor Control System

3.7.1 The 'Raspberry Pi' Computer

The Raspberry Pi is a palm sized, single board computer developed by the Raspberry Pi Foundation. It uses a Linux based operating system called “Raspbian” and during this project was used to write and run Python scripts. The board also has 26 GPIO (General Purpose Input Output) pins which can be used to interact with other electronics. These pins have a maximum output of 5V and applying more than 5V to them can cause permanent damage to the board.[15]

3.7.2 Stepper motor Drivers

Due to the complexity of their operation, stepper motors are usually controlled by a specialised circuit board called a ‘Driver’. Whilst the direction and step rate must still be specified by the computer program, the driver can alter the size of the step and the power used by the motor.

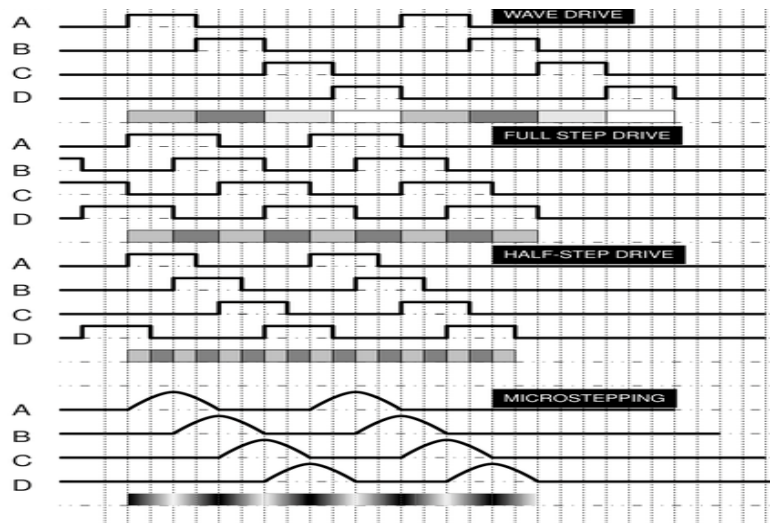


Figure 7: Stepper motor stepping options [16]

Figure 7 shows 4 possible driving configurations for stepper motors. The letters on the left hand side of the graph represent the 4 possible statuses of current flow in the 2 coils as follows:

- A = Coil 1 anticlockwise
- B = Coil 2 clockwise
- C = Coil 1 clockwise
- D = Coil 2 anticlockwise

The first three examples require square wave signalling, indicating that each coil is either powered ‘on’ or ‘off’ at any given time. Signalling patterns in which two coils are ‘on’ at all times produce the largest torques in stepper motors. The bottom of the four driving options in figure 7, labelled ‘microstepping’ requires that the voltages to various coils vary steadily over time, rather than being switched on and off. This separates each step into a number of ‘microsteps’ allowing for a more accurate angle to be achieved by the motor. A stepper driver circuit allows for the use of microstepping.

3.8 Flow around a cylinder

In order to initially validate the wind tunnel to be used in this project, it was necessary to perform a set of wake velocity measurements on a simple, standard geometry, for which drag coefficients are already known. The chosen body was an aluminium cylinder, 48mm in diameter. Fluid flow around a cylinder has been analysed in many studies, producing empirical graphs showing drag coefficients which vary with the Reynolds number of the flow based on cylinder diameter. The analysis for the flow around a cylinder can be found in the I1 report [21].

The Reynolds number, using the diameter of the cylinder as the characteristic length is given in equation 5.

Equation 5- Reynolds number based on diameter of cylinder

$$Re_D = \frac{\rho v L}{\mu}$$

Where ρ is air density, v is fluid velocity, L is the diameter of the cylinder, μ is the dynamic viscosity. A dimensional analysis of the flow past a cylinder gives equation 6, which relates the coefficient of drag to the predicted total drag force.

Equation 6 – Drag force on a cylinder

$$F_D = \frac{\rho U_\infty^2 A C_D}{2}$$

Where U_∞ is freestream velocity, A is cross sectional area of cylinder ($L \times D$). This equation was used during analysis of experimental results so far in this project to obtain theoretical drag forces for data comparison.

4 Experiment Design and Research Methodology

The research goals of the experimental group in the project were twofold. Firstly and most importantly, the real wind tunnel had to be used to obtain a set of empirical data to which the virtual data could be compared. Secondly, the reliability of this data needed to be analysed and potentially improved through modifications to the wind tunnel. Consequently, prior to any structural modifications to the tunnel, some initial tests were performed on a standard geometry (cylinder). This allowed for comparisons to be made between:

- Results found in the project wind tunnel
- Results obtained previously and discussed in the literature
- Theoretical results

Clearly the performance of a wake survey and comparison to drag forces found using CFD is a quantitative approach. However through the production of momentum loss distribution graphs and CFD streamline analysis, some qualitative comparisons between the two methods were possible also.

4.1 Initial Experiment Design

For the performance of the cylinder wake survey, both a Pitot tube and hot wire anemometry kit were available for gathering velocity data. Since the use of these two is almost identical and were interchangeable in the preliminary test rig, both velocity measurement instruments were used. This allowed for comparisons to be made between these methods and also for analysis of the wind tunnel itself. These early results were also required by the HPC subgroup for comparison to some of their early simulations.

The cylinder was chosen as the experimental body, as the theory for flow around a cylinder is well established and it is a simple geometry to mesh in CFD, making computer simulations easier and more reliable during the early stages of the project. Being prismatic makes it simpler to perform a wake survey because, as explained in section 7.1 of this report, a one-dimensional velocity profile can be taken behind the cylinder and under the assumption that the flow is also prismatic, a drag force per unit length can be calculated using Von Karman's principle and then multiplied by the required length to find the total drag force.

The methodology for the design of this initial experiment was largely influenced by the limited resources and equipment available in week 8 of the project when the testing was to be performed. The Pitot tube used was not long enough to span the width of the wind tunnel and take data for both sides of the cylinders wake, therefore the wake was assumed to be vertically symmetrical and data was collected on one side of the plane of symmetry. Clearly it is important that the whole wake of an object is studied during a wake survey, so the chosen position of the line of data to be recorded was just 10mm downstream of the cylinder and the length of the line of data points taken (width of the wake survey) was exaggerated to 3 times the diameter of the cylinder to ensure that the whole wake was definitely covered.

Attempts to record data with a u-tube water manometer proved unsuccessful as the great degree of fluctuation in the water level provided too much opportunity for human error in reading a reliable result. Therefore an automatic pressure data logger was used instead and the data was recorded on a laptop. To account for the fluctuations in pressure, an average was taken from 20 results, taken 0.5 seconds apart for each data point.

4.2 Final Experiment Design

This section explains the design process for the experiments performed using the refurbished wind tunnel with the new wake survey rig. It also details the parameters of the planned set of final experiments alongside the reasoning for those choices.

4.2.1 Final Experiment Design Methodology

The final experiment was a 2D wake survey experiment.

As explained in section 7, the final experiment was designed to make use of an algorithm developed during this project to approximate the momentum loss across plane. This algorithm requires that the wake is discretised into a square grid, on which velocity measurements must be taken. An adaptation of the trapezium rule allows the momentum loss in each grid square to be calculated separately and summed, rather than finding the total drag per length as with the typical Von Karman's formula. This allows the drag force of non-prismatic bodies, such as the concept car developed by the design group, to be calculated. Full details of the concept car development and ALM manufacture are given in [17].

When enough of the test section had been completed to test the speed achievable by the stepper motors, it was possible to calculate the amount of time required to complete any sequence of movements and thus the run time of any experiment. At maximum speed, the motors were capable of moving the assembly 5mm in just under 1 second, therefore a full second was allowed for each movement to ensure that the Pitot tube was stationary when the readings were taken by the data logger.

The precision of this method varies greatly based on two factors:

1. The resolution of the data point grid
2. The number of data taken at each point for averaging

Both of these factors will proportionately increase the time taken to complete the experiment. Since these parameters are easily changed in the python program, it was intended that a set of experiments would be performed with these values varied for comparison.

4.2.2 Refurbished Tunnel Experiment Set

It was not possible to perform all of the planned experimentation with the refurbished tunnel. It should be noted that there are significant differences between the planned final experiments and what was possible in the time available due to the unforeseeable circumstances discussed in section 2.2. However the hypothetical data sets of the planned experiments are described below and the details of the data that was actually found with the new equipment is detailed in section 7.

Firstly, an experiment would be performed to check that the timings between the probe movement system and the data logger, to check that the timings between the two stay in calibration over the course of long wake surveys. Secondly a wake survey of a cylinder would be done for comparison to results discussed in the literature review. Next a survey of the boundary layer on the floor surface would be performed, with very small increments in distance. Finally, experiments on the concept car would be iterated with variations in distance of the wake plane from the car, distance between measurements, and number of data taken at each point.

4.3 Sustainability

4.3.1 Project Energy Consumption

Since there were no consumables in the experimental portion of this project, the only sustainability concern was the use of electricity. In this section, the energy requirements of both the experimental and HPC wake surveys have been compared.

The wind tunnel operates at 480 Volts with a current of 8.4 Amps at maximum speed. This gives a power of 4.116kW. The wake survey performed by the experimental group took 1 hour 40 minutes. This gives a total energy consumption of 6.85kWh. The concept car tested in the wind tunnel was produced using a process similar to FDM (fused deposition melting), which uses 520 MJ per Kg of material deposited [18]. The car weighed 50g and therefore took 7.2 kWh of energy to produce. The computers on which the CFD calculations were performed are supplied by a 900W power supply unit. However, this is the maximum power available and it typically not required. Power consumption readings of 260W were taken for the processor during a simulation. To obtain the required result, this 1.5 day simulation was repeated 4 times, for a total power consumption of 4.68kWh.

Comparing the energy consumption of VWT use and wind tunnel wake surveys, clearly the VWT is more sustainable as it requires only 4.68kWh to obtain the data required. The ALM model and wake survey combined required 14.05kWh to create a 319 data point wake survey, although the model could be reused for further testing. Also post processing is not possible with the experimental results, whilst CFD simulations gather vastly more data per unit energy.

5 Test Section Design

5.1 Design Methodology

5.1.1 Typical Methodologies

Most commonly used design methodologies can only be applied to projects in which a number of processes can be performed at once. Such as with commercial design, or with a group of people working on the same design [19]. A commonly used design process in industry is ‘total design’, however the requirements of this go far beyond the scope of this project. Stuart Pugh, the inventor of the total design methodology, defined it as:

“Total Design is the systematic activity necessary, from the identification of the market/user need, to the selling of the successful product to satisfy that need – an activity that encompasses product, process, people and organisation.”[20]

5.1.2 Project Design Methodology

The final design of the test section and its computational control was ambitious considering the funds available and the timeframe of this project. Due to the complexity involved in the design of several linked systems, no single design methodology could be adhered to strictly. The design process was fast paced and iterative as new information regarding dimensions and specifications was becoming available daily. These constant developments across multiple systems required even small design decisions to be checked

and ensure than none of the other systems had been influenced. This included geometry analysis in Solidworks and iterations of checks against the specifications of hardware (such as the Raspberry Pi and stepper motors) to make sure that voltages and forces were not exceeded.

5.1.3 Project Design Tools

CAD (computer aided design), specifically Solidworks, was used as the main design tool for the geometry for the test section and velocity measurement instrument control mechanism. This proved at all times during the design process, that there would be no collision of parts during wake surveys and that everything lined up as it needs to. It also allowed for fast creation of part drawings for use in the workshop. Secondly, several parts of the test section were made by university workshop technicians. Their expert consultation was invaluable designing a product which would work and was possible to manufacture in the available timeframe.

5.2 Old Test Section Condition

5.2.1 Initial State

It was clear that the old test section had been used for a number of different experiments over several years, as there were many ports and holes cut into the sides, presumably as either pressure taps or access for flow measurement instruments. The flanges, top, bottom and back were made from 15mm thick MDF (Medium Density Fibreboard) and the front (and circular top plug) were made from Polymethylmethacrylate (PMMA)

This section was fine for the initial testing but due to the extent of the planned modifications, it was decided that it would be rebuilt entirely. The initial test section (adapted for use in the preliminary experimentation of this project), can be seen in figure 4. The dilapidated state of the tunnel was not only aesthetically unappealing but also a detriment to its functionality in certain respects. For example, the scratched and clouded Perspex on the front face made smoke visualisation streamline analysis less clear and any uncovered ports in the walls will create uneven flow conditions.

5.2.2 Modifications for Testing

In order to make the initial test section suitable for the planned preliminary tests, some simple modifications were made to it and a guide mechanism was built for the Pitot tube. As can be seen in figure 8, both sides of any holes in the section were covered in electrical tape to keep the tunnel air tight. The main hole covered in this picture was 40mm in diameter. This is because the pressure drops as the flow speed increases and would case air to enter the tunnel through these holes, disturbing the flow.



Figure 8 – Photographs of the initial test rig

The rig shown in the photographs (Figure 8) was manufactured to provide a set of wake velocity data for any prismatic body placed vertically in the flow. It consists of a removable piece of the Perspex test section wall, a Pitot tube, guiding boss and ruler.

5.3 New Test Section Design

In this section the design is explained and decisions are justified for the test section and measurement equipment positioning system.

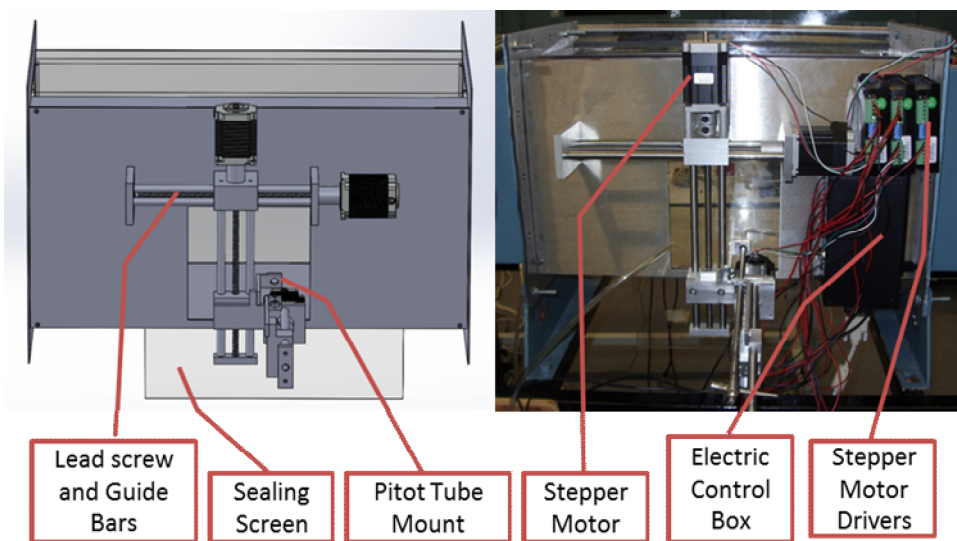


Figure 9 – Diagrams shows the components of the Pitot tube positioning system on both the CAD model (left) used during its design and the finished product (right).

5.3.1 Velocity Measurement Instrument ‘Control Mechanism’ Design

This design of this system was split into two key design areas:

1. The support mechanism, responsible for guiding the path of the instruments and providing a structure to support the positioning system.

2. The positioning system, which would move the instruments through the degrees of freedom defined by the support mechanism, to the required positions for measurements.

Concept design for the new section began in week 9 of the project (November 2013), including initial sketches of the translation mechanism for the Pitot tube positioning system. Evidence of alternate designs can be found in the appendix of the I1 Report. [21]

5.3.1.1 Manual Positioning System Considerations

As discussed in section 5.4.1, in order to obtain the required set of data, the automated positioning system would have to move to split second timings for 1 hour and 40 minutes. These timings would be impossible to achieve through manual movement without creating the possibility for large human errors. That is not to say that the system could not be driven manually. In the initial tests it was proven that using stopwatch timing, the Pitot tube could be positioned manually using human judgement to maximum (human) accuracy within 10 seconds.

If the positioning system on the new test section were to be manually operated, then measures would be taken to ensure than the precision were improved over that of the initial tests. The use of electronic callipers would allow for tolerances of just 0.01mm, however the amount of time taken to get the position exactly right using manual mechanical methods was potentially more than 10 seconds, meaning that the 1 hour 40 minute automated data set would take more than 3 hours to perform manually. If a full three dimensional wake survey were performed, it would take 80 hours manually and only 30 hours automatically.

Also, due to the unavailability of the wind tunnel outside of working hours, performing long experiments manually would be impractical. An 80 hour manual experiment is equivalent to 10 working days or 2 work weeks (due to unavailability on weekends). Whereas automatic systems could easily run overnight without the insurance liabilities which arise due to personnel present after hours. Therefore what would take 2 weeks to achieve manually, could be achieved in 1 day, 6 hours automatically.

Due to the complexity of the test section and the consequent workload, it was decided that a positioning system would be developed which was automatically driven, but could be disconnected from the driving system and to allow manual operation through the use of a mechanical crank. Therefore if it became apparent that the automated system could not be completed in the required timeframe, then the system could be operated manually to obtain a set of data to ensure that the validity of the VWT could be assessed.

5.3.1.2 Automated Positioning System Design

The maximum speeds attainable in linear actuators are governed only by the motor power, internal friction and external loading. However with stepper motors, attempts to increase step speed past a certain point will result in jamming as the core of the motor does not complete its step before current is switched to the next phase. Instead of the core being forced further in the desired direction, it will move in reverse to the closest opposite pole.

In this sense, linear actuators are better but there are other factors to consider in the choice of motors than speed. Since the speed of a linear actuator is dependent on the load applied to it, without constant measurement it is impossible to know its exact position. Approximations can be made as to the current required to move a certain distance however, any small errors will likely accumulate over time causing large inaccuracies for complex wake surveys. This can be remedied through the use of ‘encoders’ which are essentially feedback systems. Laser systems can be used to repeatedly check the position of a linear actuator against the position that it is supposed to be in, as defined by the program. Stepper motors can achieve far superior positioning accuracies even without a feedback loop. This saves time, money and complexity in the system, consequently, Nema 23 stepper motors were chosen for the automated positioning system.

5.3.1.3 Translational Support Mechanism

The choice of measurement instrument motion path is important as it dictates the shape of the data set available in the tunnel.

Firstly, a translational motion was chosen over rotation as it allowed for the creation of identically sized and shaped cells. This meant that in the calculation of drag forces the only variable was the fluid velocity. The use of irregular cells would also cause variation in cell resolution and thus reliability throughout the data set, cells closer to the pivot would be smaller than those further away.

Secondly, since it had been decided to automate the motion, it was logical to design the movement mechanism with three degrees of freedom to allow the collection of 3D data sets. The alternative to this was only to automate the X and Y axis, and manually change the Z axis to reduce complexity. This would work fine for wake surveys of bodies from which the shape of the wake is known, however as discussed in section 7, a wake survey is not appropriate for wakes in which the flow is not parallel to the free stream. Performing wake surveys at different distances from the tested body provides evidence as to whether the wake is approximately unidirectional (the resultant flow momentum loss should be the same). As long as the whole wake is measured, then the loss of momentum in the flow should be equal regardless of the distance from the body.

5.3.1.4 Perspex Sealing Screen

The final component was the perspex screen designed to move with the positioning system and keep the 170mm x 170mm hole in the back of the tunnel sealed. Without this, the wind tunnel would be unusable as there would be a large flow inlet at the side of the tunnel. This screen is just large enough to allow the measurement instrument to reach all four corners of the square hole, taking a complete 140x140x140 mm wake survey, without allowing significant flow through the side of the tunnel. The screen moves between 2 identical stainless steel sheets which keep it in place, and it is sealed both sides with felt.

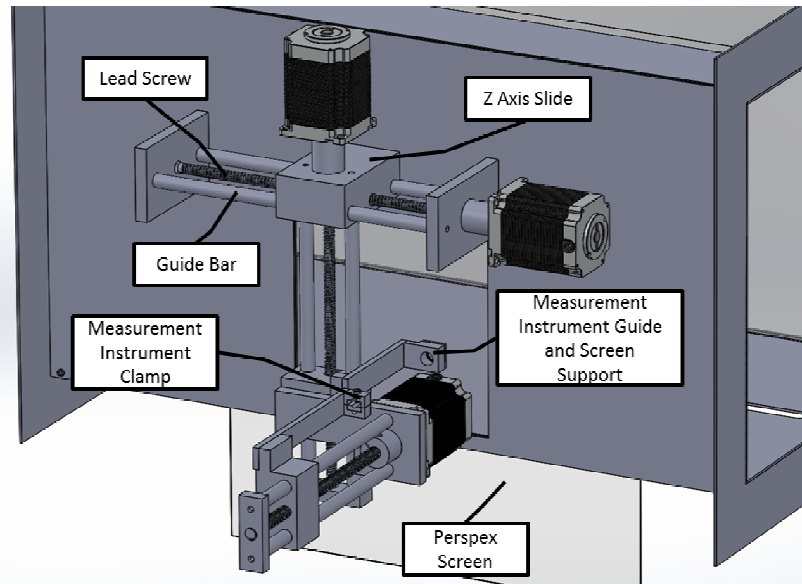


Figure 10 – Labelled Solidworks model of the final test section design.

5.4 Electronic System Design

5.4.1 Python Script Design

Driving a stepper motor requires the driving current to be switched between two circuits within the motor at a rate proportional to required movement speed. Control of the motors was simplified through the use of stepper motor driving circuits. To control these stepper motors, a 24 volt, 3 amp power supply was required, which was not directly possible due to the 5V limitation on the Raspberry pi GPIO ports. A program was written in Python code on the Raspberry Pi to control the movement of the Pitot tube in three axes. The program begins by counting down from three in the display, with a comment instructing the user to start the data logging system on ‘GO!’. This is because the two systems are not linked and must be started simultaneously. Incorrect timings between the two systems would result in the measurements being taken whilst the Pitot tube was in motion. Subsequently, the program controls the GPIO ports on the Raspberry Pi to create a square wave voltage signal to the stepper motor drivers. Exactly 1000 waves correspond to a linear movement of 5mm in the translational positioning system, this is called the pulse signal. A second ‘direction’ signal was also controlled by the program. This is a constant ‘on or off’ signal which represents whether the stepper motor should turn clockwise or anti clockwise. These two signals are sent in an order which corresponds to the required motion of the three stepper motors.

5.4.2 Electronics Hardware

The electrical system consisted of the following components:

- Raspberry Pi computer
- 3 x ‘M524’ stepper motor drivers
- 3 x ‘Nema 23’ stepper motors
- 24V 3A stepper driver power supply unit – mains connection
- Computer monitor
- Raspberry Pi power supply unit

- Emergency stepper driver 8A toggle switch

The majority of the small, loose components were assembled within a black plastic box to protect them and arrange them to make wiring and connections simple. Holes were cut in the box to allow connecting wires to be plugged in from the sides. A photograph of the control box containing all components is shown in figure 11.

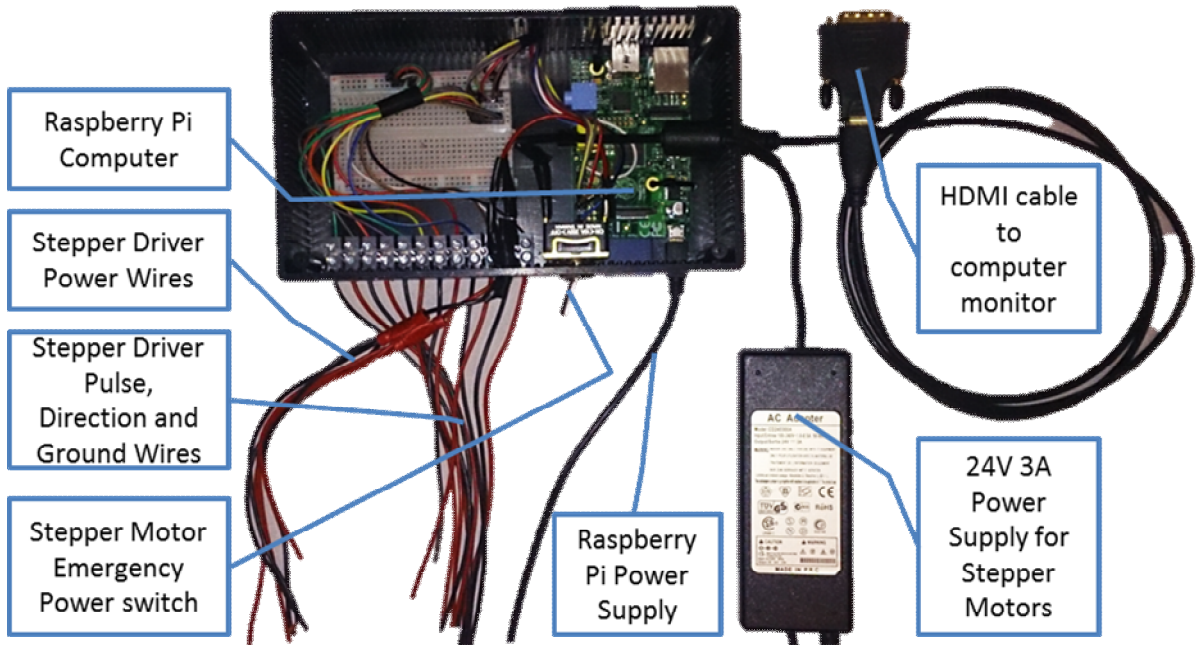


Figure 11 – Photograph of the test section electrical control box, components and connections are labelled

External from this box were the stepper motors and their drivers. Wires were arranged on the test section in such a way that they would not be stretched or hinder the motion of the mechanism.

5.5 Wind Tunnel Section Design

Clearly the dimensions of the interior of the test section structure were predefined by the rest of the tunnel, however the materials were not. Stainless steel was chosen for the main shell as it is strong enough, even when as thin as 2mm. This makes it quicker to work with and to weld than thicker, mild steel. To improve the use of flow visualization methods within the tunnel, it was decided that the top and front would be transparent. The top surface was made from 8mm thick Perspex as it was held in place by screws, however the front surface was made of one sheet of removable glass. Glass is much more difficult to scratch than Perspex, and is likely to stay clearer for longer. Due to the structural weakness of the Perspex-glass edge, a mild steel bar was used to bridge this gap and keep it sturdy.



Figure 12 – Photographs of front and top of test section

6 Experimental Methods

6.1 Gathering Useful data

As stated in the I1 report [21], one of the objectives of the experimental group was to gather data to prove/disprove the usefulness or viability of the virtual wind tunnel. The obvious approach was to choose a value which could be calculated using both systems and analyse the difference in result. Aerodynamic drag is attainable through CFD and through the use of both velocity measurement and of a drag balance in a real wind tunnel. During the project, a drag force was found using each of these three methods. This allowed for two comparisons to be made.

6.2 Initial Experiment Method

In the initial set of experiments, both a Pitot tube and a hot wire anemometer were used to find a velocity profile for the flow around a cylinder. Two people were required to perform this experiment. The first (the mover) was responsible for moving the Pitot tube to the correct position between data recordings; the other (the timer) was responsible for calling out the timings. The data logger used could not be programmed to take irregular intervals. Therefore, to ensure that the results taken whilst the tube was in motion could not influence the results, the experiment was split into 10 second increments. During the first 10 seconds, the first 20 results (for averaging) would be recorded for the first data point, after which the timer would indicate that the tube could be moved over the following 10 seconds. During the third set of 10 seconds, 20 results for the second data point were taken, and so on until the entire wake had been measured. A diagram of the experiment is given below in figure 13.

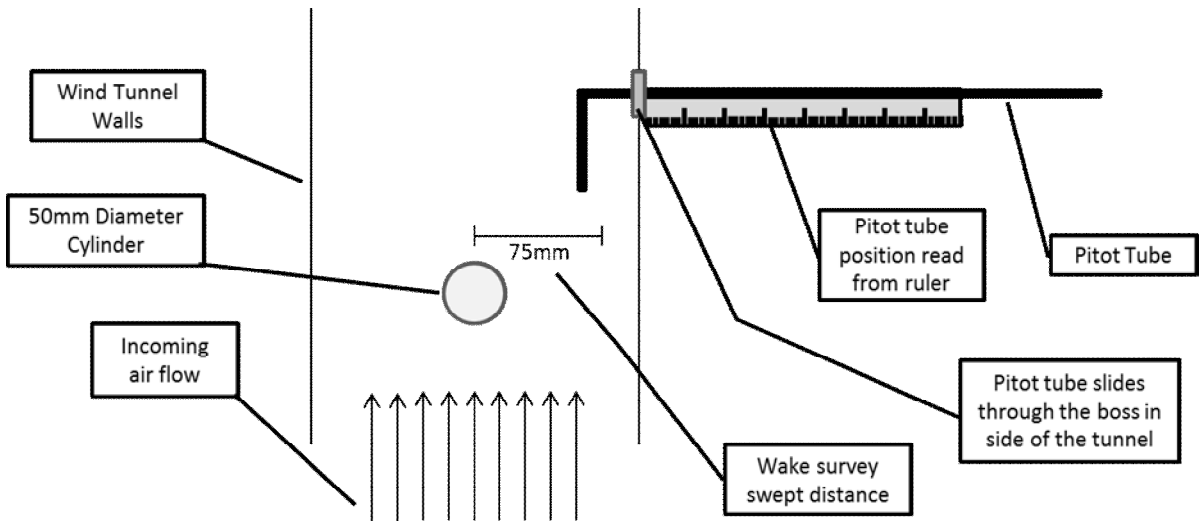


Figure 13 – Diagram of initial Pitot tube experiment on a cylinder wake

6.3 Final Experiment Method

Due to the numerous setbacks described, the manufacture of several parts, along with the reassembly of the wind tunnel were done in the final week of laboratory availability. This only left several hours on the final day (28th march) to connect the Raspberry Pi to the mechanical system, test both systems and gather data for the validation of the wind tunnel. Consequently, a three dimensional wake survey was not possible. There were several minor issues with the mechanical system which could have easily been solved if the time had been available.

The Final experiment employed the new test section took a wake survey 80mm from the rear of the car. The shortness of time caused the following problems:

1. The Z axis (direction parallel to flow) motor was left unconnected to save time, as it would not be used in a two dimensional wake survey. Consequently the survey plane could not be moved closer or further from the car. Since a Pitot tube was being used to measure the flow velocity, it was important that its tip was sufficiently far from the concept car to ensure that vortices off the car did not cause flow to move over the Pitot tube at an angle. This, combined with the use of the new, longer Pitot tube, pushed the position of the concept car far back towards the inlet of the tunnel as shown in figure 14.
2. Due to the placement of the car being so close to the inlet, it could not be positioned in the centre of the tunnel as it was obstructed by the pulley used in the drag balance experiments. Therefore the car was placed adjacent to the pulley so it was as close as possible to the centre of the tunnel.
3. Finally, as a consequence of the off centre positioning of the concept car, the anchoring cable (previously the drag balance cable), was attached to the car at an angle of 14° to the flow. The force in the cable along with the reaction force of the pulley pressing on the side of the car, created a moment which twisted the car in line with the anchor cable as soon as the wind tunnel was turned on. This is shown in figure 14.

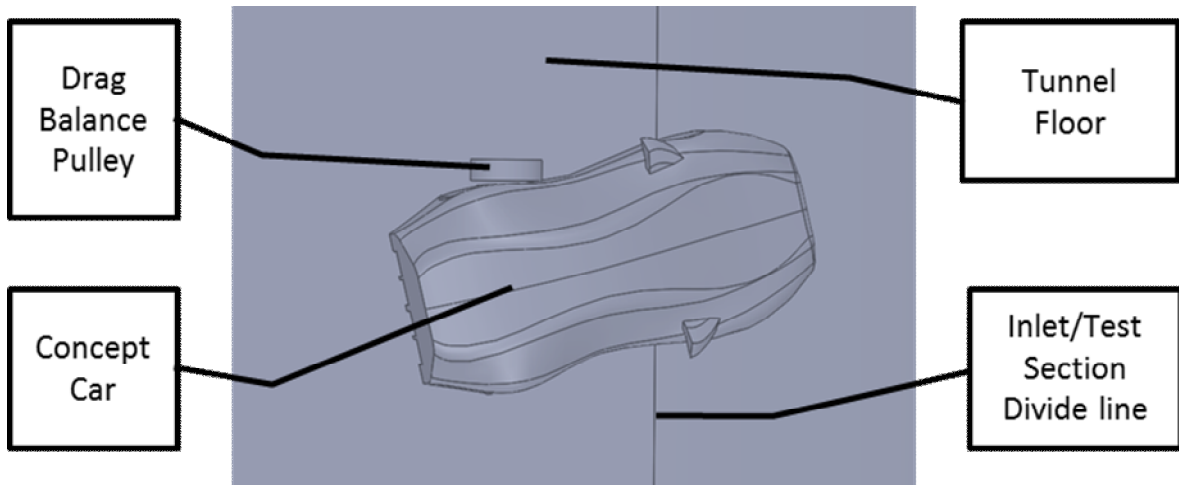


Figure 14 – Solidworks model of the concept car position during the wake survey experiment

In this experiment, the resolution was set to 5mm for the sake of consistency with the initial test and 3 data were taken at each position in the grid from which a mean average was taken.

Although the test section was capable of three-dimensional wake surveys, only a two-dimensional survey was performed, again due to time constraints. A three-dimensional wake survey with 5mm increments in the Z axis would take 30 hours to complete. With just two dimensions this time is reduced to 1 hour and 40 minutes. Only 50 minutes were available for testing, but as much data as possible was collected in that time.

The python program moves the Pitot tube through a full sweep in the X axis (140mm normal to the sides of the tunnel in 5mm increments), before moving 5mm in the Y axis (normal to the bottom of the tunnel) and repeating the X axis sweep. In 50 minutes, a wake survey 140mm wide and 50mm high was achieved with 3 measurements taken at each point for averaging.

7 Results and Analysis

7.1 Initial Experiment Findings (old test section)

Both Pitot tube and hot wire anemometer wake surveys were performed on the wake of a cylinder. The data and full analysis of these experiments is given in the I1 report [21]. This section describes the findings of these experiments and what was changed in the final experiment method to achieve more favourable results.

The data collected during the initial experiments was highly erroneous. The results predicted negative drag in some areas of the wake survey (the flow had been accelerated). In other regions of the flow, the results predicted very large drag values when compared to theory. Through analysis, it was decided that this was for one of three reasons.

1. The pressures in the tubes connected to the Pitot-static tube may not have been correctly calibrated. This could have led to an increased measured velocity for the whole wake survey.

2. When choosing the size of a body for wind tunnel testing, is it important that the size of the tunnel is considered. A general rule for wind tunnel experimentation is that the cross sectional area of the tested body is at maximum, 10% of the cross sectional area of the tunnel. This is due to the fact that if there is too large an obstruction, then the flow will be forced to accelerate past the body as it has significantly less area to pass through [22]. After the initial experiments showed flow acceleration, the cross sectional area of the cylinder was measured and found to be 16% of the cross sectional area of the wind tunnel. The flow acceleration would have resulted in the appearance of negative drag readings.
3. A Pitot-static tube 4mm in diameter was used for the initial tests. When the data was being collected, it was noticed that at certain positions in the cylinder wake, the tube would vibrate significantly from the force of the flow. This may have been responsible for the negative drag calculations as the lateral movement of the Pitot tube could have caused a perceived flow velocity component in the direction of the side ports. These ports should not experience kinetic flow forces if accurate results are to be achieved. If the pressure readings in these side ports increased significantly, then the calculated dynamic pressure would have been much lower, resulting in the appearance of lower flow velocity. Combined with 1 and 2, this could have contributed to the negative drag readings.

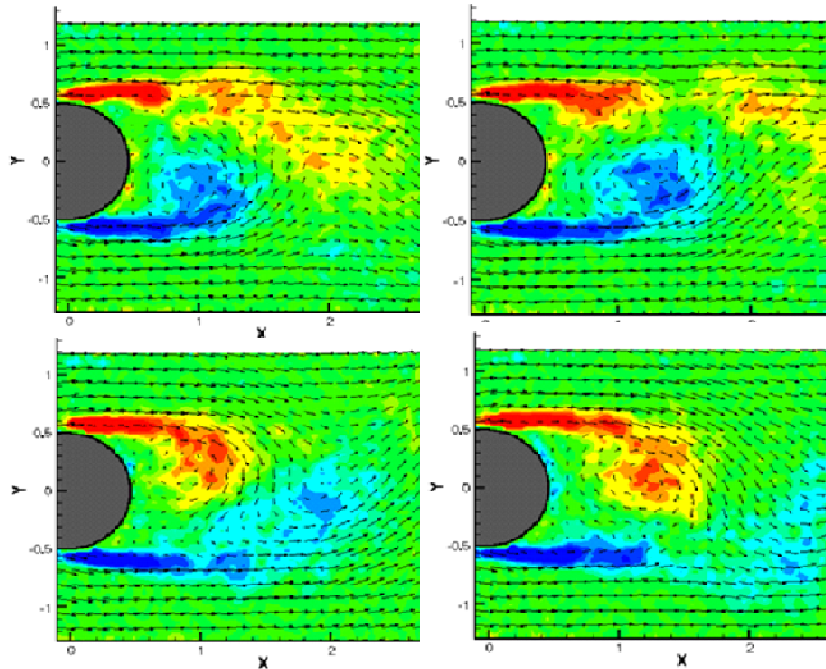


Figure 15 – CFD graphs of velocity vectors throughout the cycle of alternating vortices around a cylinder. Cycle order: Top left, top right, Bottom left, Bottom Right. [9]

It may also be the case that a cylinder is not an ideal geometry for this experiment. From the CFD velocity vector plots given in figure 15, is it clear that the alternating vortices cause flow in all directions, including perpendicular to the flow (which would add kinetic forces to the static port readings) and reverse flow which would explain the negative pressures observed in the measurements in that region. From this it can be determined that only certain bodies are suitable for wake survey study as Pitot tube use requires approximately unidirectional flow. It may also be possible that the results could have been improved by taking a wake survey further downstream to allow the flow to settle its

direction. This is reinforced by the hot wire anemometry data obtained, which was also erroneous. Hot wire probes are not affected by the direction of the flow (to the same extent) and similar, low velocity results were observed.

From this initial study, several conclusions were drawn about improvements to be made in the design of the final experiment. Firstly, the wake survey was to be taken at a variety of distances from the body to compare the wakes close and further downstream. Theoretically, assuming the whole wake is covered within the survey control volume, the calculated drag should be identical at any distance. Secondly, a larger, sturdier Pitot tube would be used and calibrated correctly. This would remove the chance of further vibrations during testing and of large systematic errors from poor ‘zero’ level pressures. Finally, it would be ensured that the cross sectional area of the concept car was less than 10% of the cross sectional area of the wind tunnel test section.

7.2 Final Method Experiment Data Processing

From the final wake survey, the Pitot tube data logger recorded 1650 data. Since this is too much data to manually process through multiple calculations, an excel spread sheet was designed to process this data set and any future wake surveys of the same dimensions. The following is a summary of the algorithm performed by the spreadsheet:

1. Firstly, the user must copy the static and total pressures in the html file measured from the two ports on the Pitot tube. These are pasted into the designated area on the spreadsheet and the pressure data is aligned in two columns by the program, adjacent to the first ‘Time’ column. The program then calculates the dynamic pressures by subtracting the static from the total pressure. These are recorded in a fourth column.
2. The data recorded whilst the Pitot tube was moving was invalid, therefore the valid data had to be separated from the invalid data prior to further processing. This was achieved through the use of a ‘valid/invalid’ column in which all rows containing valid results contained the number ‘1’ and all invalid rows were left blank. This allowed for the use of the ‘sort’ function within excel to separate them. The validity of each line of data was determined through analysis of the timings in the python script.
3. The valid results were then split into their sets of three (as three measurements were taken at each point). The mean average was then taken for each point in another column.
4. Using the formula below, the pressures were converted to velocities. The value for density ‘ ρ ’ was taken as air at 20°C but can be changed by the user. Due to the square root over this equation and the inability of the following calculations to process complex numbers, any negative pressure differences had to be disregarded. This is discussed in section 7.3.4.

$$v = \sqrt{\frac{2(P_t - P_s)}{\rho}}$$

5. Since data is required for every point for the drag calculations, any negative data were replaced by approximations, found by interpolating between the two adjacent velocities assume a linear relationship between the three points. In the case of the data set obtained for the concept car, only two results were replaced by these approximations.
6. Once a set of velocities had been obtained for each of the 319 points in the 140mm x 50mm grid, the data was tabulated. Next, the table was arranged to place the velocity data into groups of four, separating the 5mm x 5mm individual areas.

Using a user defined free stream velocity, the quantity ' $U_x(U_\infty - U_x)$ ' was calculated for each point in a similar table. This created a surface on a 3D graph with the X and Y axis for the X and Y position of each data point and the Z axis for ' $U_x(U_\infty - U_x)$ '. The volume bounded between this surface and the plane 'Z = 0' was equal to the total loss in momentum.

7. In order to find this volume, a form of numerical surface integration was performed in which the volume under each 5mm x 5mm surface was found separately. One of these volumes can be exemplified in figure 16.

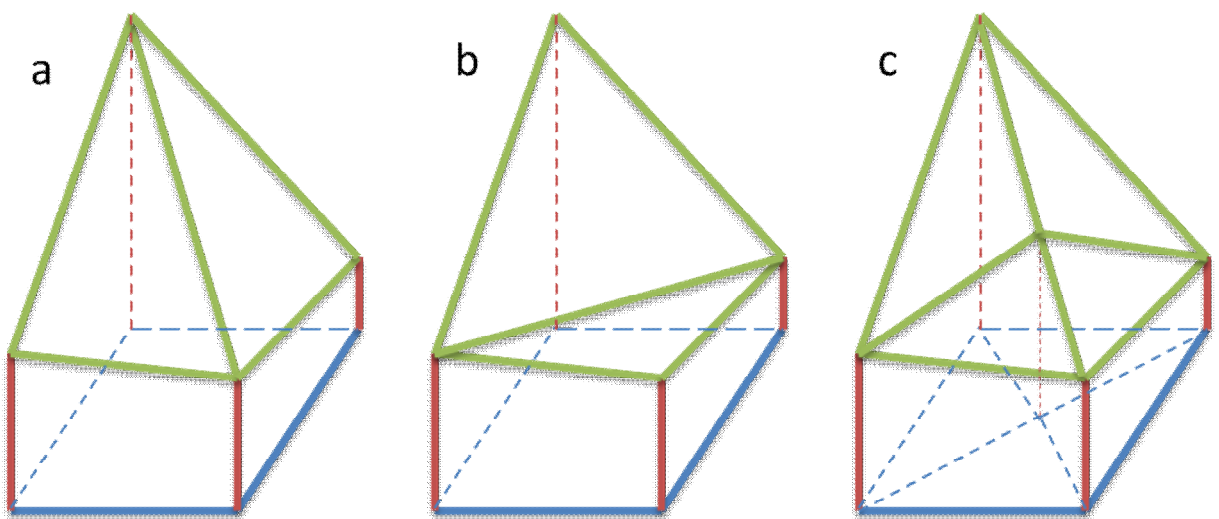


Figure 16 - Diagrams of the same hexahedron top surface split through both diagonals

8. Each of these hexahedra does not necessarily have one unique volume, as the top surface may be either convex or concave depending on which way the diagonal line is placed, as shown in figure 16 (a,b). The only cases in which they only have one possible volume are where the sum of the lengths of the opposing edges are equal ($A+C=B+D$), which gives the top of the shape a flat surface. It was decided that arbitrarily deciding a direction in which to place the diagonal in every case was not ideal, as it may lead to large systematic errors when surveying wakes which vary diagonally. Instead for each hexahedron, a 5th point was added in the centre at a height equal to the mean of outer 4 points, splitting it into 4 triangle based, irregular prisms. as shown in figure 16 (c). The data was then rearranged into another table which splits it into the sets of 5 velocity data which make up each

hexahedron (and 4 triangular prisms). An example of this table is displayed in table 3.

Table 3 – Example section of the calculation spreadsheet. Each 3x3 cell area (coloured) calculates the drag in one hexahedron. The 4 corner values are the recoded data and the centre value is the mean average.

	0.0	2.5	5.0	5.0	7.5	10.0	10.0	12.5	15.0
0.0	29.39		33.53	33.53		36.68	36.68		38.16
2.5		31.76			34.24			37.25	
5.0	33.36		30.77	30.77		35.99	35.99		38.16
5.0	33.36		30.77	30.77		35.99	35.99		38.16
7.5		32.59			34.08			36.51	
10.0	31.66		34.58	34.58		34.98	34.98		36.91
10.0	31.66		34.58	34.58		34.98	34.98		36.91
12.5		31.90			33.59			35.90	
15.0	31.30		30.04	30.04		34.74	34.74		36.98
15.0	31.30		30.04	30.04		34.74	34.74		36.98
17.5		28.50			30.69			34.45	
20.0	25.01		27.64	27.64		30.32	30.32		35.76

9. The volume of each of these triangular prisms was found using the formula in equation 7.

Equation 7 – Volume of an irregular triangular prism

$$\frac{B(a+b+c)}{3}$$

Where a,b and c are the heights of the three sides and B is the area of the base, as shown in figure 17. Unlike with the hexahedra, the volume is always defined.

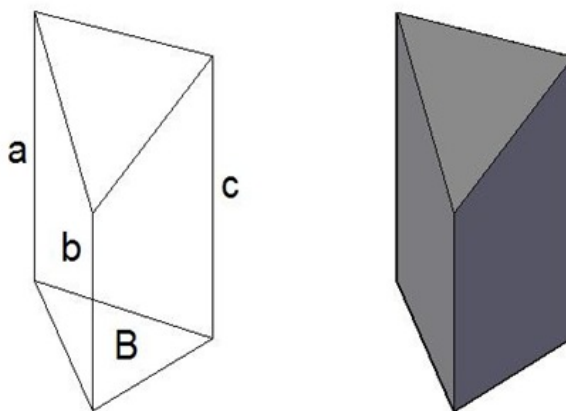


Figure 17: Labelled diagram of an exemplar irregular triangle based pyramid, for which the volume is calculated in equation 7 [23]

10. The volumes of each hexahedron were found by summing the respective four triangular prisms. These volumes are equal to the number of newtons of flow momentum loss per m^2 of the wake
11. These volumes were summed to give the total momentum loss over the whole wake, equal to the drag force on the concept car. $F_D = 1.19 \text{ N}$.

This spreadsheet is available on the CD in appendix 4. Currently it is specific to wake surveys of 140mm x 50mm, however it could be easily adjusted to perform the same calculations on larger wakes. Written instructions are provided within the spread sheet regarding its use.

7.3 Final Method Results Analysis

7.3.1 Comparison to Drag Balance Experiment

In this section, the data of the 140mm x 50mm wake survey of the concept car is studied to make judgements about its validity and about potential inaccuracies in the experimental procedure or the wind tunnel itself.

The Drag force found using the wake survey method, detailed in section 6.3, was $F_D=1.19\pm 0.25 \text{ N}$. This gave a drag coefficient for the concept car of $C_{D\text{WakeSurvey}}=0.358\pm 0.077$. Since the car was at a slight angle to the flow during testing, the frontal profile (thus area) was different to that of the drag balance experiments conducted by Docherty [24], in which the car was straight, shown in figure 18. Therefor the two set of experiments could not be compared directly as this largely affects the drag coefficient.

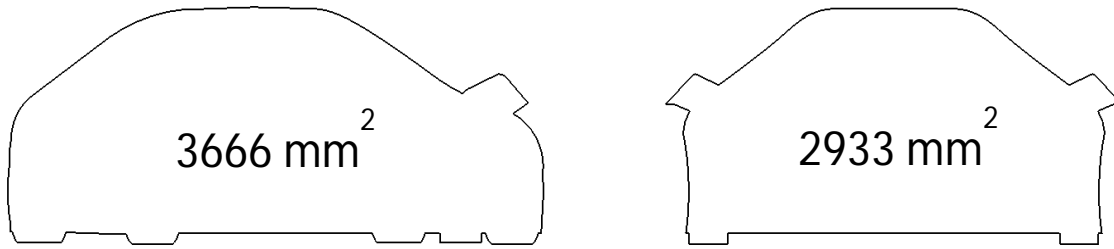


Figure 18 – Silhouette outline of the frontal profiles (with respect to the flow direction) of the concept car during the wake survey experiment (left) and the drag balance experiment (right), labelled with the corresponding frontal areas.

7.3.2 Tunnel Floor Boundary Layer

Figure 19 shows a graph of the momentum loss over the whole of the measured wake. The drag for each 5mm x 5mm square area is represented at a single point in the centre of the square.

Three Dimensional Plot of Momentum Losses in the Wake Survey

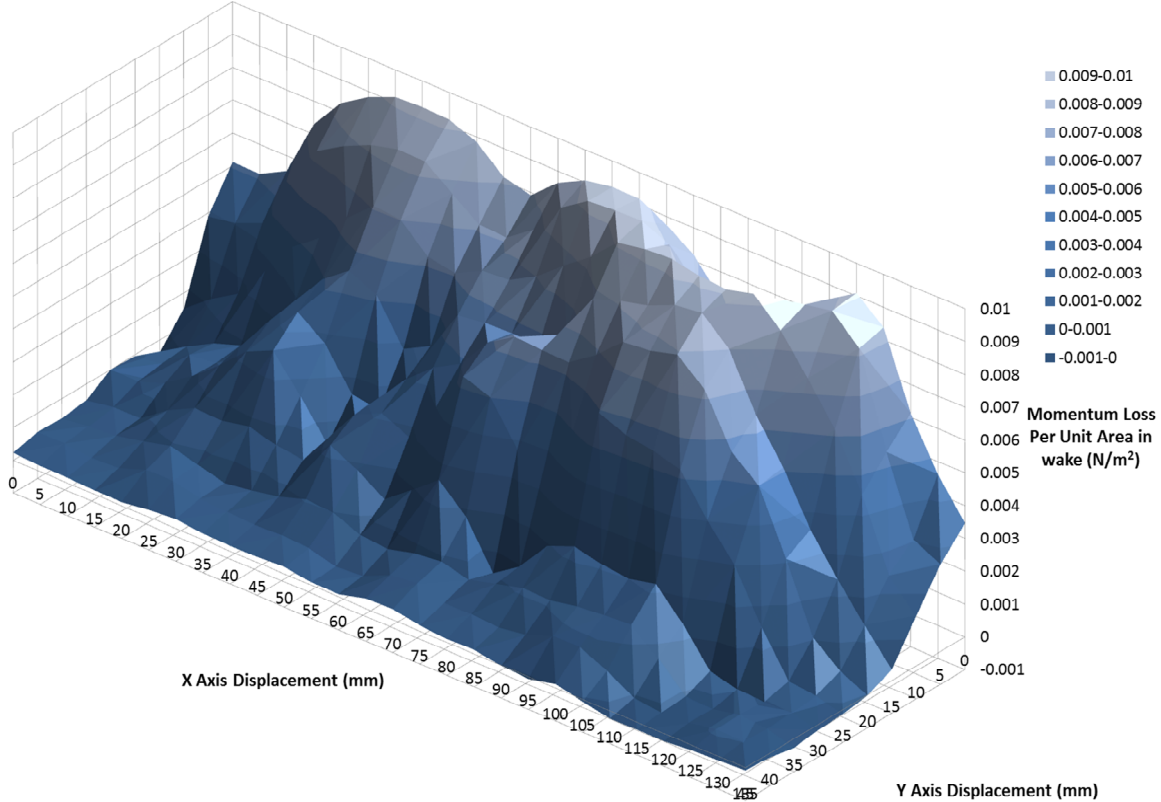


Figure 19: Graph showing a 3D surface plot of momentum losses over the wake survey area

The first thing to note from this graph is the wake of the car is apparently not completely covered in the wake survey area. All three edges (the fourth being the floor of the tunnel) of the wake survey would be at free stream velocity, and therefore would have no momentum loss, if the whole wake were within these boundaries. However, where the Y axis displacement is below 15 and at the extremes of the X axis, there were still significant momentum losses recorded. Since the Y axis displacement is the distance of the Pitot tube from the floor of the wind tunnel, some of this “momentum loss” could be explained by the presence of the boundary layer forming on the tunnel floor plate. In actuality, it would not be momentum loss in the boundary layer region, but rather an error in calculation due to the fact that the same free stream velocity was assumed for all positions in the flow upstream of the body.

The flow may not have slowed down close the tunnel floor to produce the perceived drag effects in that region, but because it was slower than free stream velocity to begin with, it was considered (by the calculations) to have lost momentum.

This could be accounted for in two ways:

1. The Velocity profile of the boundary layer could be measured without the presence of the concept car and the calculations adjusted to treat the free stream velocity as a function of Y axis displacement, rather than as a constant.
2. The momentum loss in the boundary layer could be approximated and subtracted from the total value.

It was not possible to take a velocity profile of the boundary layer, again due to time constraints and laboratory unavailability, thus an approximation was made using CFD. In the wake survey experiment the concept car model was on the intersection between the test section and the inlet. To simplify the problem, the boundary layer was modelled as a flat plate assuming that it would have developed similarly over the smooth curve of the inlet. Taking velocity readings in a line out from the plate in small increments, a velocity profile was obtained and then the trapezium rule and the Von Karman integral formulation were used to find the momentum loss from the discrete data. This was the same process as was performed to find the wake survey of the cylinder in the initial experiments discussed in the I1 report. The calculated momentum loss due to the presence of the boundary was 0.524 N.

This boundary layer momentum loss could be subtracted from the total drag force found in the wake survey experiment, however this is not a true representation of the effect of the boundary layer, as the loss of flow momentum is not linear. This means that the real boundary layer flow will slow down less as it passes over the body than the freestream flow would, so the result should not be directly subtracted.

The theoretical boundary layer thickness was then calculated. The position of the concept car during the wake survey experiments was at the connection between the inlet and test section. This means that the boundary layer encountered by the car had developed over the curved surface of the inlet. For the purpose of the following calculations, the inlet was modelled as flat plate again. Firstly the Reynolds number of the flow at that point was calculated with equation 8. The characteristic distance was the length along the plate, 700mm.

Equation 8 – Reynolds number, based on the characteristic distance ‘x’[12]

$$Re_x = \frac{Ux}{v}$$

Where Re_x is the Reynolds number, U is the freestream velocity, x is the characteristic distance and v is the kinematic viscosity of air (9.49×10^{-6}). This gives $Re_x = 2.8 \times 10^6$. Theoretically the boundary layer is turbulent when the Reynolds number is above 5×10^5 , so the boundary layer in the tunnel was considered turbulent. [25] From this Boundary Layer thickness was calculated using equation 9.

Equation 9 – Turbulent boundary layer thickness [12]

$$\delta = \frac{0.382x}{Re_x^{0.2}}$$

Where δ is the boundary layer thickness. The boundary layer was calculated to be 13.7mm thick. Comparing this value to figure 19, it is very possible that the wake survey did cover the whole wake of the concept car as the flow momentum loss approaches 0 between 13mm and 15mm from the tunnel floor.

7.3.3 Comparisons to CFD Data

Due to the rushed nature of the wake survey experiment, the exact position and angle of the car could not be measured and given to the HPC group to use in the VWT. The position used for calculations was obtained through analysis of photographs taken during the experiment. The exact position was to be measured the following week when the lab re-opened however by this time, the car had been accidentally destroyed by university cleaning staff. This is likely to have two effects on the comparisons between experimental and CFD results. Firstly, the two sets of results may have a translational difference, meaning that the graphs would not ‘line up’ but the total drag should be approximately the same (assuming that the majority of the wake is still covered). However more importantly, if the angle of placement is incorrect, then the drag forces could be different altogether.

The Reynolds-averaged Navier-Stokes (RANS) are a time-averaged version of the Navier-Stokes equations which consider flow properties as a summation of the property’s mean flow and its turbulent fluctuations [26]. On the other hand the experimental results were taken as a mean average of 3 readings taken 1 second apart. Since the fluctuations in velocity occur over fractions of a second (approximately 0.1 seconds according to detached eddy simulations [27] , the time resolution of the experimental data was not nearly small enough to create a reliable average velocity at each point. The fluctuations averaging in RANS allows the production of a seemingly fluctuation free wake survey, whilst many more data would need to be recorded at each position to achieve the equivalent through experimentation for comparison.

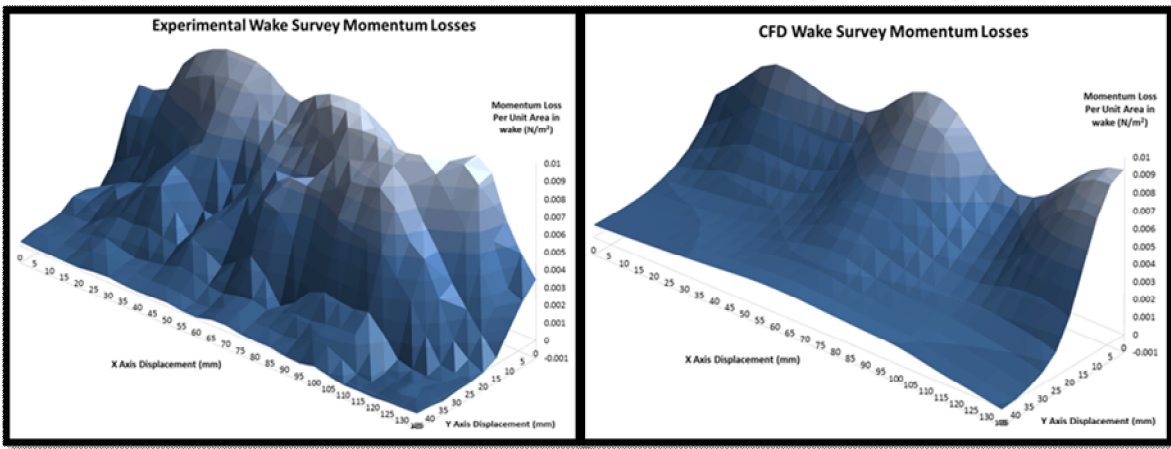


Figure 20 - Side by side comparison of experimental and CFD wake surveys

Figure 20 shows a comparison between the wake surveys in the experimental results and those found in RANS CFD results [27]. To create the equivalent CFD graph, 319 probes were placed in the RANS simulation to create a set of data identical to that of the experimental wake survey. The velocities obtained were put through the same algorithm as the experimental data.

The resultant drag force in the CFD data was 1.03 N, compared to the experimental result of 1.19 ± 0.25 N. From this drag force, the drag coefficient in the CFD case was calculated at 0.310 compared to the experimental value of 0.358 ± 0.077 . It could be stated that the results are in agreement, as the error bar of the experimental result encompasses the CFD result, however 21% error in the experimental result is too high to say this with any certainty.

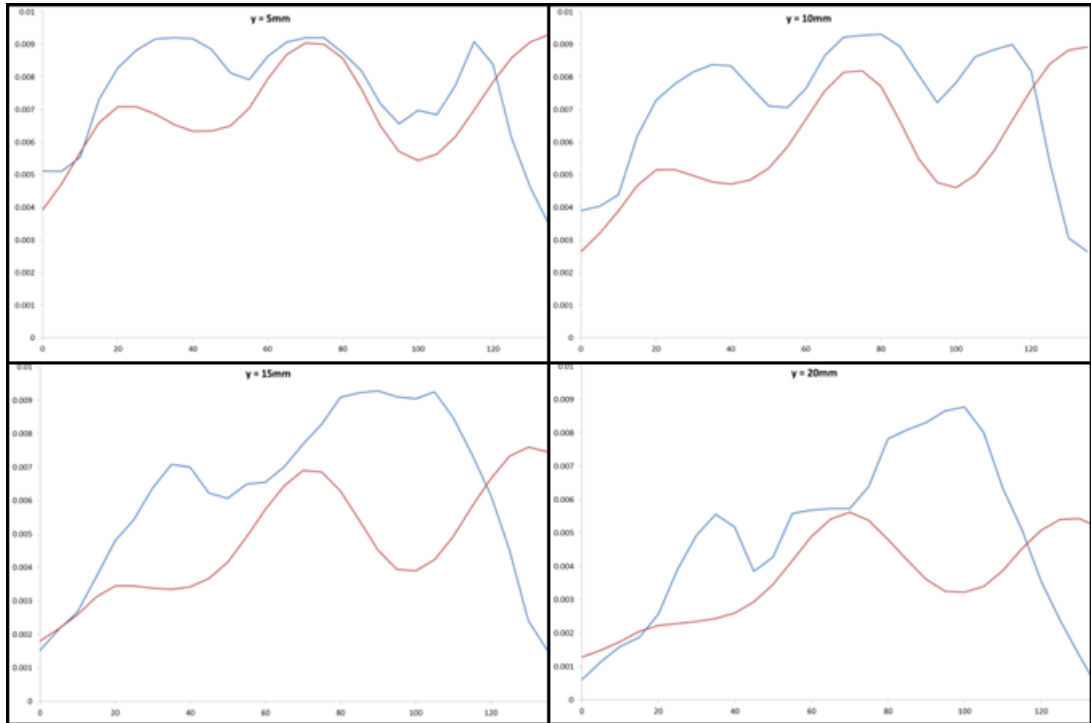


Figure 21 - Graphs showing the comparison between experimental and CFD wake study velocity plots in the x axis, at distances of 5, 10 15 and 20mm from the tunnel floor

Figure 21 shows four one-dimensional wake survey comparisons between computational and experimental results, taken from the two-dimensional survey. From these it seems that the approximated position of the CAD model was correct in terms of translational positioning, but may not be at the exact same angle as the experimental case.

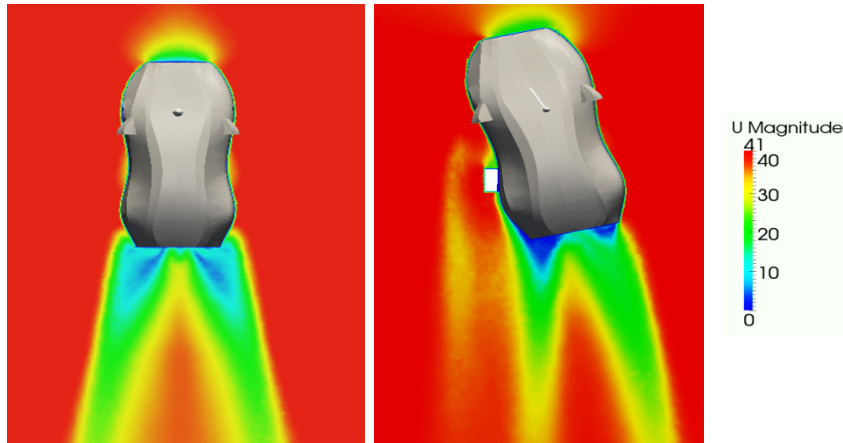


Figure 22 – CFD contour plots of the velocity in the wake of the concept car. The ideal test scenario with the front of the car facing the flow (left) and the CFD replication of the experimental conditions with the car angled at 14° [27] (right).

This can be explained by studying the contour plots of velocity around the concept car shown in figure 22. In both situations, there are large velocity losses behind the rear wheels of the car. However for the angled car, there is a third stream of lessened velocity behind the left wing mirror. This helps to explain the increase in drag force and the car is angled and clearly explains why the drag balance experiment produced a much lower drag coefficient by comparison.

These three low velocity streams are responsible for the three peaks in the wake survey data in figure 20. The correct translational position of the car in the CFD model is proven by the vertical alignment of the middle peaks in the data at $y = 5\text{mm}$. This data is also in reasonable agreement in the two side peaks. However, the further the flow from the plate, the less agreeable the side peaks are, until $y = 20$ where the only agreeing peak in the central one. This suggests that the cars' angle was incorrect in the CFD simulation by a small amount, as the centre peak relates to the highest point of the car, at which the flow is most obstructed.

7.3.4 Error Calculation

Only three data points were taken at each position, so performing accurate statistical analysis is not possible, however, efforts were made to quantify the error of these measurements. For each mean average of 3 data, the difference between each measurement and its relative mean was calculated. These were summed and divided by the total number of data points and the average distance of any given data point from its mean was 8.91m/s . This corresponds to an error of 21.4% in the drag force and drag coefficient.

These errors are most likely due to random fluctuations in the velocity of the flow. Despite the large error, the drag forces calculated with CFD and through experimentation were relatively close. This may be explained by the law of large numbers, which describes how the repetition of an experiment a large number of times is likely have an average close to the correct value [28]. If the fluctuations are random, then they are just as likely to be higher velocities as lower velocities. The combination of 1650 random contributions and deductions from the drag force may have averaged out to be roughly the same.

8 Future Work

8.1 Program Development

The programs required to control the position of the flow velocity measurement instruments was written during term 2. By this point it was becoming clear that this section of the project would be pressed for time for the reasons described in the mitigation information dossier in the appendix of this report. Consequently, only a simple program was written to run the single wake survey experiment. If the program were to be developed, it should be checked that it is in timing calibration with the measurement system. Also, the values such as step size and size of the wake survey could become input commands allowing a fully customisable wake survey, although this would be difficult to match with the calculation spreadsheet.

8.2 Further Experimentation for the validation of the VWT

In order to more closely match the RANS VWT case, a similar wake survey should be attempted with a much tighter resolution and with many more data taken at each position for a more reliable average. Also, 3 dimensional wake surveys of the concept car should be performed to check that the entire wake was measured. The momentum loss of the flow should be identical at any distance from the car as long as the whole control volume is captured.

8.3 Further Tunnel Improvements

8.3.1 Boundary Layer Reduction

As mentioned in the results section, the tunnel used for this project could also benefit from a boundary layer reduction system. Industrial wind tunnels tend to make use of flow injection / removal to manipulate the pressures in the boundary layer. However, without significant investment into pumping hardware and serious alterations to the current tunnel, this would not be possible. The most realistic and effective potential solution is to build a small rolling road on which to place the model car. The rolling road would be set to move at the same speed as the free stream velocity and consequently, the flow adjacent to it would not be disturbed [29]. Since the project wind tunnel is likely to be used for purposes other than automotive design, this may not be practical.

8.3.2 Smoke Removal

As discussed in the wind tunnel literature review, the use of smoke in an open return tunnel results in the accumulation of smoke in the laboratory. To increase the usefulness of this tunnel, either the tunnel, or its positioning in the room should be altered to decrease the rate of smoke release. The following are concepts developed during the project, but could not be implemented due to time constraints or logistics.

1. The simplest solution is to move the tunnel to a position in the lab where the exhaust can be directed into a vent or out of a window.

2. If the tunnel is to maintain its position in the laboratory, an extension of the exhaust could direct the smoke through a hole in the outside wall, ejecting the entire flow from the room. 4.05 m^2 of air passes through the tunnel every second at full velocity of 45 m/s .
3. Finally, a separate, smaller exhaust could be placed in the flow downstream from the body but upstream from the propeller. Although not all of the smoke could be removed, a large proportion could be if the exhaust were placed in the right position. Consequently, a much smaller exhaust hose would be required and the clean air would exit the tunnel normally.

8.3.3 Turbulence Screen

In contrast to many of the open return wind tunnels studied during the design process, the project wind tunnel does not have a turbulence screen over the inlet to stabilise the flow and reduce turbulence. This means that any of the inlet flow conditions discussed will be worsened. Since only a mesh screen or array of vanes is required in the manufacture, it is recommended that a screen be applied to the tunnel for future testing

9 Conclusions

This project has achieved two key deliverables to a high standard. The wind tunnel test section has been improved and the virtual wind tunnel results have been validated, albeit with high error data.

Firstly, the wind tunnel test section designed and built during the project functioned exactly as it should, fulfilling all specifications set out in the I1 report [21]. Whilst not all of its functions could be made use of during the project, it is still capable of performing fully automated three-dimensional wake surveys and provides a clear view of the tested body for any future flow visualisation experiments.

Secondly, the test section was used to analyse the drag profile of the concept car. This experimental data was compared to a CFD case with the same conditions. The drag coefficient was calculated for each case, the CFD predicted 0.310 and the empirical result was 0.358 ± 0.077 . Whilst these figures do concur to a degree, more experimentation would need to be performed to improve the reliability of the wake survey before solid conclusions could be drawn about the validation of the virtual wind tunnel.

Thirdly, through comparison between the experimental wake survey and the CFD velocity contour plots, the origin features of the drag peaks were identified. This would allow for concept car optimisation if the project were to continue.

Finally a number of recommendations have been made for future work:

- Development of the python program to increase its versatility
- Further experimentation with the new test section to obtain more reliable data
- A number of further modifications could be made to the wind tunnel to improve its function and wake survey accuracy such as a turbulence screen, boundary layer reduction and smoke removal hardware

10 References

- [1] Lockyer, K.G., Gordon, J. 1991. Critical path analysis and other project network techniques, 5th ed. Pitman. pp. 236.
- [2] Anderson, J.D., 1999. Introduction to Flight, 4th ed. McGraw-Hill Science/Engineering/Math.
- [3] Graebel, W.P., 2001. Engineering Fluid Mechanics. Taylor and Francis. pp. 386.
- [4] Browand, F., 2005. Reducing Aerodynamic Drag and Fuel Consumption. Available online at:
http://gcep.stanford.edu/pdfs/ChEHeXOTnf3dHH5qjYRXMA/10_Browand_10_11_trans.pdf Accessed 29/04/2014
- [5] Bradshaw, P., et al. Wind tunnel design Available online at:
<http://navier.stanford.edu/bradshaw/tunnel/diffuser.html> Accessed 29/04/2014
- [6] Recirculating wind tunnel pic, Available online at:
<https://www.grc.nasa.gov/www/k-12/airplane/tuncret.html> Accessed 29/04/2014
- [7] Schlichting, H., Gersten, K., 2000. Boundary-Layer Theory. 8th ed. Springer.
- [8] Audi thermal wind tunnel info. 2014 Available online:
<http://www.audi.com/corporate/en/research-and-technology/wind-tunnel-centre/thermal-wind-tunnel.html> Accessed 29/04/2014
- [9] Merzkirch, W., 1987. Flow Visualisation. 2nd ed. pp. 25.
- [10] Wake survey instrument Image, Available online:
<http://www.khi.co.jp/corp/asmb/test-j/wake.html> Accessed 29/04/2014
- [11] Open return wind tunnel image,
<http://discoverarmfield.com/es/products/view/c15/tunel-de-viento-controlado-por-ordenador> Accessed 29/04/2014
- [12] Fitzpatrick R, 2012 Derivation of Von Karman Integral Formulation Available Online: <http://farside.ph.utexas.edu/teaching/336L/Fluidhtml/node89.html> Accessed 29/04/2014
- [13] Lomas, C., 1989, Fundamentals of hot wire anemometry, Cambridge University Press.
- [14] MacDonald G, Stepper Motor Function Diagram, Stepper Motor Control with the Raspberry Pi, Full video available at:<http://www.youtube.com/watch?v=Dc16mKFA7Fo> Accessed 29/04/2014
- [15] Raspberry Pi Foundation, Raspberry Pi – Model B [computer], 2014.
- [16] Wikipedia article: Stepper Motors, Available online
http://en.wikipedia.org/wiki/Stepper_motor Accessed 29/04/2014

-
- [17] Browne, F., 2014. Individual Report I2: Virtual Wind Tunnel Project. MEng Report. University of Exeter
- [18] Baumers M, Tuck C, Bourell DL et al. *Sustainability of additive manufacturing: measuring the energy consumption of the laser sintering process*. IMechE Part B: J Eng Manuf 225:2228–2239
- [19] Description of common design methodologies, 2012 Available online at: http://www.nwlink.com/~donclark/design/design_models.html Accessed 29/04/2014
- [20] Pugh, S., 1991. Total Design. Addison-Wesley Pub. Co.
- [21] Blades, L., 2014. Individual Report I1: Virtual Wind Tunnel Project. MEng Report. University of Exeter
- [22] González Hernández, M. A, Moreno López, A. I, Jarzabek, A. A, Perales Perales, J. M, Wu, Y, and Xiaoxiao, S., (2013) Design Methodology for a Quick and Low - Cost Wind Tunnel. INTECH. [online] Available at: [intechopen.com](http://www.intechopen.com), last accessed 21/4/2014
- [23] Irvine, D., Mathematics blog, available online: <http://darrenirvine.blogspot.co.uk/2011/10/volume-of-irregular-triangular-prism.html> last accessed 21/4/2014
- [24] Docherty, D., 2014. Individual Report I2: Virtual Wind Tunnel Project. MEng Report. University of Exeter
- [25] Kothandaraman, C. P, & Rudramoorthy, R (1999) Basic Fluid Mechanics. New Delhi: New Age International Ltd.
- [26] 2014. Group Report G2: Virtual Wind Tunnel Project. MEng Report. University of Exeter
- [27] Hamilton, L., 2014. Individual Report I2: Virtual Wind Tunnel Project. MEng Report. University of Exeter
- [28] Wikipedia Article: Law of large numbers, Available online at: http://en.wikipedia.org/wiki/Law_of_large_numbers Accessed 21/4/2014
- [29] Farrell, T., 2003, Development of a New Boundary Layer Control Technique for Automotive Wind Tunnel Testing, Available online at: <http://soar.wichita.edu/bitstream/handle/10057/760/t05051.pdf?sequence=1>